Title

ACCLIMATION OF PHOTOSYNTHESIS TO THE ENVIRONMENT 1 regulates Photosystem II Supercomplex dynamics in response to light in *Chlamydomonas reinhardtii*

Short title

Photosynthetic electron transport regulation

Marie Chazaux[1], Stefano Caffarri[1], Juliane Da Graça[1], Stephan Cuiné[1], Magali Floriani[2], Pawel Brzezowski[1*], Gilles Peltier[1], Bernard Genty[1], Jean Alric[1] and Xenie Johnson[1+]

[1]Aix Marseille Univ., CEA, CNRS, Biosciences and Biotechnology Institute Aix-Marseille, Saint Paul-Lez-Durance, France F-13108

[2]Institut de Radioprotection et de Sûreté Nucléaire (IRSN), PRP-ENV/SRTE/LECO, Cadarache, Saint-Paul-Lez-Durance, France F-13108

*present address: Humboldt Universität zu Berlin, Institut für Biologie, AG Pflanzenphysiologie, Berlin, Germany

+corresponding author. xenie.johnson@cea.fr

The author responsible for distribution of materials integral to the findings presented in this article in accordance with the policy described in the Instructions for Authors (www.plantcell.org) is: Xenie Johnson (xenie.johnson@cea.fr).

Abstract (170 words)

Photosynthetic organisms require acclimation mechanisms to regulate photosynthesis in response to light conditions. Here, two mutant alleles of *ACCLIMATION OF PHOTOSYNTHESIS TO THE ENVIRONMENT 1* (*ape1*) have been characterized in *Chlamydomonas reinhardtii.* The *ape1* mutants are photosensitive and show PSII photoinhibition during high light acclimation or under high light stress. The *ape1* mutants retain more PSII super-complexes and have changes to thylakoid stacking relative to control strains during photosynthetic growth at different light intensities. The APE1 protein is found in all oxygenic phototrophs and encodes a 25 kDa thylakoid protein that interacts with the Photosystem II core complex as monomers, dimers and supercomplexes. We propose a model where APE1 bound to PSII supercomplexes releases core complexes and promotes PSII heterogeneity influencing the stacking of Chlamydomonas thylakoids. APE1 is a regulator in light acclimation and its function is to reduce over-excitation of PSII centres and avoid PSII photoinhibition to increase the resilience of photosynthesis to high light.

Introduction

In plants, algae and cyanobacteria, photosynthetic electron transport is tightly linked to light capture and CO_2 assimilation. Depending on light intensity and CO_2 availability, either the light reactions or carbon metabolism will be limiting for photosynthesis (Farquhar et al., 1980). Balancing the two results in poising the electron carriers along the chain from the Photosystem II (PSII) electron acceptors (plastoquinones) to the Photosystem I (PSI) electron acceptors (Fd, FNR, $NADP^+$). This energetic balance must be constantly tuned to environmental cues in order to avoid over-reduction of the photosynthetic apparatus and photo-damage. Referred to as photosynthetic acclimation, it involves both fast regulation of thylakoid proteins as well as slower, long-term changes to light harvesting and photosystem stoichiometry (for reviews see (Anderson et al., 1995; Erickson et al., 2015; Walters, 2005)).

PSII is the water splitting primary reaction component of the electron transport chain of oxygenic photosynthesis. It is a highly conserved multi-subunit complex composed of pigments and proteins which first evolved in cyanobacteria, the progenitor of chloroplasts (Caffarri et al., 2014). The PSII reaction centre (RC) is made up of D1 and D2 proteins that contain the co-factors required for charge separation, heme b_{559} (bound to PsbE and F), and the inner antenna of the core, CP43 and CP47 (Bricker and Ghanotakis, 1996). The PSII core complex includes the RC plus the oxygen evolving complex, PsbO, PsbP and PsbQ (Thornton et al., 2004). Additionally, around 20 other low MW proteins are observed in the homodimeric crystal structure and are required for PSII dimer or supercomplex stability (Caffarri et al., 2009; Umena et al., 2011). Many more proteins have been found to interact with PSII transiently in substochiometric quantities with precise functions to optimize oxygen evolution, electron transfer, PSII stability, protection or repair. These extrinsic proteins contribute to the flexibility and stability of PSII during periods of environmental variation or during biogenesis (Komenda and Sobotka, 2016; Plochinger et al., 2016; Shi et al., 2012). Efficient PSII regulation and repair is a necessity because PSII contains chlorophyll excited states that can react with locally produced oxygen. During repair, the turnover rate of D1 protein can be very high while electron transfer remains functional: this is achieved by dynamic changes involving the heterogeneity of PSII complexes (Guenther and Melis, 1990; Jarvi et al., 2015; Kirchhoff, 2019).

Large antenna complexes are required to efficiently capture the light energy for transfer to the PSII core. In all phototrophic eukaryotes, the light harvesting complex II (LHCII) proteins that are rich in chlorophyll *b* (chl *b*) and account for most of the pigments associated with PSII perform this role. The LHCII antennae attached to a PSII core form a PSII supercomplex (PSII SC) and this association can take different oligomeric forms and is determined by environmental conditions (Bielczynski et al., 2016; Shen et al., 2019; Su et al., 2017). Regulators LHCSR3 and PsbS, bind to the antenna of PSII SC and down regulate light harvesting by promoting non-photochemical quenching (NPQ), a safe dissipation of light energy as heat (Correa-Galvis et al., 2016a; Correa-Galvis et al., 2016b; Nawrocki et al., 2020; Semchonok et al., 2017; Tibiletti et al., 2016). State transitions change the functional antenna size of PSII whereby the phosphorylation status of the LHCII adapts antenna cross section of both PSI and PSII to the redox state of the electron transport chain (Dumas et al., 2016). Such quenching and photoprotection mechanisms are considered to be short-term acclimation processes (Erickson et al., 2015).

At the supramolecular level, PSII is embedded in thylakoid membranes of eukaryote phototrophs. Similar to plants, in unicellular green algae, PSII are mostly found in more stacked regions of the thylakoids while PSI are found in non-appressed lamellae and margins (Goodenough et al., 1969; Goodenough and Levine, 1969; Goodenough and Staehelin, 1971; Kouril et al., 2018). However, PSII is heterogeneous both in its distribution in the thylakoids and in its supramolecular organization. PSII SC are found in the grana stacks while PSII core complexes can also localize to margins and stromal lamellae (Albanese et al., 2016; Boekema et al., 1999; Danielsson et al., 2006; Drop et al., 2014; Koochak et al., 2019; Schwarz et al., 2018; Suorsa et al., 2015). These organizations are dynamic and thylakoids adapt their structure in response to light. In low light, thylakoids form stacks of highly dense membranes containing PSII SC, a structure favoring light capture (Polukhina et al., 2016; Rochaix, 2014). PSII forms semi-crystalline ordered arrays (Boekema et al., 2000) and high molecular mass assemblies containing numerous LHCII and forming megacomplexes across the stromal gap (Albanese et al., 2017; Albanese et al., 2016; Boekema et al., 2000; Wei et al., 2016). In high light, thylakoid membranes become less stacked and the number of layers decreases. This change can be as fast as a few minutes after the transition from low to high light (Rozak et al., 2002).

Destacking of thylakoid membranes is accompanied by PSII antenna size adjustments and changes to the density of SC, which corresponds to the long-term acclimated structure in response to the higher light intensity (Bielczynski et al., 2016; Kouril et al., 2013; Polukhina et al., 2016). Destacking allows for damaged PSII core complexes to disassemble into PSII core dimers, PSII core monomers and Repair Complex 47 (RC47: PSII core monomer lacking CP43) and facilitates migration towards the non-appressed lamellae and grana margins. Changes to stacking and reduction in antenna size of PSII prevents oxidative stress (Herbstová et al., 2012; Khatoon et al., 2009) and is also required for PSII repair (Jarvi et al., 2015; Theis and Schroda, 2016)

In eukaryote oxygenic phototrophs, the acclimation response to an increase in light intensity is defined by three major factors: a decrease in the relative abundance of thylakoid membrane to stroma, decrease in relative chlorophyll content and an increase to chlorophyll *a/b* ratio (Melis, 1996). With higher light the requirement for light harvesting is reduced, while the photosynthetic yield increases in line with electron transport and CO_2 assimilation rates relative to the lower light intensity (Anderson et al., 1995). *Acclimation of Photosynthesis to the Environment 1* (*ape1*) allele was initially identified in a screen in *Arabidopsis thaliana* to identify mutants affected in the long-term light acclimation responses that are linked to increasing photosynthetic yield (Walters et al., 2003). At*ape1* did not increase PSII quantum yield after a shift to high light. During acclimation to strong light, the Chl *a/b* ratio increased in the wildtype, but not in At*ape1,* indicating that the high light response of increasing PSII core (rich in chl *a*) and decreasing LHCII antenna (rich in chl *b*) was active in the wildtype but affected in At*ape1* (Walters et al., 2003). This preliminary characterization pointed to a role for APE1 in an unknown but major light acclimation mechanism, but neither the mechanism nor the protein was further studied.

Using *Chlamydomonas reinhardtii* as a model organism, we present a characterization of high light acclimation and we demonstrate that the *ape1* mutant phenotype is deficient in this process. We have determined APE1 localization, interactions, and function in regulating light capture and photoprotection at the level of PSII. We propose that APE1 plays a role in the remodeling of PSII SC, thereby regulating electron transport for CO_2 fixation and preventing PSII photoinhibition.

Results

APE1 maintains photosynthetic growth in high light

In the context of deepening our knowledge on light acclimation processes, we isolated a mutant in Chlamydomonas with poor photosynthetic growth at high light affected for variable chlorophyll fluorescence under these conditions (Figure 1)(Figure 1A, B, C). Using a PCR-based technique we identified the left-flanking region of the insertion site of the antibiotic resistance cassette in the 3'UTR of the *Cre16.g665250* locus, annotated as *Acclimation of Photosynthesis to the Environment 1* (*APE1*, www.phytozome.jgi.doe.gov, v12.1.5). Sequencing of the insertion site showed that 1.5 copies of the *APHVIII* cassette are present (Supp. Figure 1). RT-PCR of the *Cre16.g665250* locus in this mutant showed presence of *APE1* transcript, not unexpected for an insertion in the 3'UTR (Figure 1D). This allele was designated *ape1-1* after successive outcrossings and backcrossings to a wild type 137cc strain.

We also obtained a second allele from the CLiP library (Zhang et al., 2014), annotated as having an insertion in intron 4 of *Cre16.g665250*, and designated LMJ.RY0402.039504. The insertion site (Supp. Figure 1) was confirmed by PCR. RT-PCR analysis revealed no transcript for *APE1* (Figure 1E). The obtained mutation was successively crossed into our wildtype line and we named this allele *ape1-2*.

The two alleles *ape1-1* and *ape1-2* cells grew equally well as the wild type at 5 and 40 $\mu mol_{photons}.m^{-2}\ s^{-1}$ heterotrophically (see TAP in Figure 1A); on the contrary both *ape1-1* and *ape1-2* showed impaired growth in high light (at 300 $\mu mol_{photons}.m^{-2}\ s^{-1}$), especially on minimal medium (see the dilution series, Figure 1B). Addition of 2% CO_2 in the growth chamber allowed the mutants to grow like the wild type. These observations seemed to assign to *APE1* a role in acclimation of oxygenic photosynthesis in response to light and CO_2 availability.

Complementation of *ape1-2* line using the WT copy of APE1 under the control of its native promoter resulted in a complemented line (*ape1-2* c2) with improved phototrophic growth in high light compared to the *ape1-2* mutant (Figure 1C).

Chlorophyll fluorescence imaging showed that the maximum quantum yield of PSII (F_V/F_M) was very low in the mutant (~ 0.19) but it reached the WT (~ 0.35) value in the complemented line (~ 0.39).

Immunoblot analysis using the antibody against APE1 showed that this protein was reduced to around 5-10% of the wild type level in *ape1-1,* but it was absent from *ape1-2* (Figure 1F and G). The APE1 protein accumulation is restored to WT levels in three independent *ape1-2* complemented lines, which correlates with the improved growth characteristics (Figure 1C). The complemented line *ape1-2* c2 is referred to as *ape1-2*:APE1 in the experiments below.

APE1 is a primordial thylakoid protein

The *APE1* gene model can be identified exclusively in oxygenic phototrophic organisms (Figure 2)(Figure 2A). APE1 has homologues in all cyanobacteria strains sequenced, including in *Gloeobacter violacelus* that lacks thylakoid membranes (Rexroth et al., 2011). It is however not found in any anoxygenic phototrophic species, bacteria containing only one of either type of reaction center (*Chloroflexus aurantiacus*, RCII or *Heliobacillus mobilis*, RCI). Supplemental Figure 2 shows representative species used for the hypothetical protein alignment used for the Cladogram. The predicted gene product shares 34-38% sequence identity with 17 homologs in these oxygenic phototrophs.

The *APE1* gene of *C. reinhardtii* is predicted to encode a 25 kDa mature protein, modeled using RaptorX: http://raptorx.uchicago.edu/ (Kallberg et al., 2012) (Figure 2B) with two hydrophobic helices on the N-terminus (predicted as transmembrane helices by TMPred) and a soluble domain of unknown function (Domain of Unknown Function 2854) which constitutes the majority of the protein and is unique to APE1 (Supplemental Figure 2). The *C. reinhardtii* APE1 has a predicted chloroplast transit peptide of 41 amino acids (predicted by PredAlgo, giavap.genomes.ibpc.fr).

The APE1 antibody was used to determine APE1 protein localization. APE1 is present in the chloroplast, in the isolated thylakoid fraction, shown by immunoblot analysis. APE1 was present with thylakoid PSAD, while it was absent in the stromal

fraction, where Rubisco accumulated (Figure 2C). APE1 is thus a chloroplast thylakoid protein with origins at the beginning of oxygenic photosynthesis.

APE1 contributes to the accumulation of PSII proteins and LHCII antenna but is not required for biogenesis

To quantify possible differences in the accumulation of PS proteins, we analysed thylakoid proteins isolated from WT and *ape1-2* grown in low light heterotrophically. Proteins were separated using gradient denaturing gels and resolved using the highly sensitive SYPRO staining technique (Figure 3). Immunoblot analysis shows that APE1 cannot be separated from LHCII in this analysis (Figure 3A). PSII proteins D1 and D2 were quantified using Image J and found to accumulate less than the WT while LHCII proteins accumulate more than the WT (by approximately 20% in both cases). Other core and minor antenna appeared unaffected using this technique (Figure 3A). Immunoblot analysis shown for *ape1-1* grown phototrophically at low light (80 $\mu mol_{photons}.m^{-2}.s^{-1}$) showed a similarly reduced PSII content for D1 and here the other PSII proteins tested were also reduced when compared against the wild type (Figure 3B). The accumulation of major photosynthetic complexes did not show major differences when respective protein content was compared. Photosynthetic parameters for cells grown under these conditions showed that the quantum yield of PSII was not significantly different in *ape1* from the control strains (Supp. Table 1).

When multi-subunits chloroplast complexes are not properly assembled, they are degraded, and when a dominant subunit of a complex is missing, the synthesis rate of the other subunits is reduced by the mechanism of “control by epistasy of synthesis” (Choquet et al., 2001). In *ape1-1*, APE1 barely accumulates (Figure 3C). In mutants devoid of PSII (*psbA*) and PSI (*psaB*), grown hetrotrophically, APE1 content was similar to the wild type. These results show that APE1 is not an intrinsic subunit of the photosystems and is not strictly required for their assembly.

The accumulation of the APE1 protein was also tested in both low and high light phototrophic culture conditions (Figure 3D). APE1 was quantified and found to accumulate to the same amount in both conditions. However as opposed to accumulation of APE1 in Figures 1, 2 and 3C showing protein samples from

heterotrophically grown cells in low light, in figure 3D, APE1 migrates not as one band but as two bands and they accumulate in different quantities between low and high light phototrophic conditions. Taken together these results show that APE1 protein accumulates constitutively and may also be modified post-translationally depending on the media or the light intensity.

APE1 interacts with PSII core complexes

The sequence analysis of APE1 and the low PSII quantum yield of *ape1* in high light suggested a functional link to PSII activity and we next performed experiments to identify protein-protein interactions with native photosynthetic complexes. Mild solubilization of purified thylakoid membranes with 0.5% digitonin/ 0.5% α-DM followed by separation of protein complexes by BN PAGE (4-16%) was followed by immunoblot analysis of D1 and PsaD to identify PSII and PSI complexes. It gave five bands for PSII: two SC forms, of which one also contains PSI, the PSII core dimers, the PSII core monomers and RC47 (PSII Reaction Center with CP47 but without CP43). Four bands of varying intensity were identified for PSI (Figure 4).

Immunoblot with APE1 antibody did not show any cross-immunoreaction against thylakoid proteins other than APE1 (see *ape1-2* lane, Figure 4B). APE1 migrated mostly with the higher molecular mass fractions (megacomplexes, aggregates or non-solubilized membrane fragments) as well as the low molecular weight fraction. In between these two extremes, defined bands were obtained at the same level of D1, showing that APE1 co-migrated with PSII SC, PSII dimers and monomers, but not the PSII repair fraction, RC47. Neither, did APE1 co-migrate with the trimeric antenna fraction. In BN PAGE (4-16%) there were at least two bands where PSI and PSII co-migrate or migrate very closely to each other.

Therefore, we tested for APE1 accumulation in complexes from mutants devoid of PSI (Δ*PsaB*) or PSII (Δ*PsbA*) and using BN PAGE (3-12%) and silver-stained 2D gels (Figure 5)(Supplemental figure 3). As in Figure 4B, APE1 was found below and above LHCII trimers, probably as aggregates. In Δ*PsaB*, APE1 was detected in two specific bands, PSII core monomers and dimers that are absent from the Δ*PsbA* lane. This result unambiguously shows that APE1 co-migrates with the PSII core, with monomers and dimers.

To prove an interaction with PSII, protein crosslinking was tested using glutaraldehyde (GA) (Figure 6). Thylakoid membranes were solubilized in 1% α-DM and 1% Digitonin and loaded on sucrose gradients, with or without GA and subjected to ultracentrifugation. The sedimentation profile was not significantly changed whether the crosslinking agent was added or not (see Figure 6A), showing that, under these conditions, GA did not affect the fractionation into SC. Seven bands were collected and their absorbance was measured to control the content in photosynthetic complexes. All of the B5-B8 fractions contained PSII, the B5 fraction peaked at 675 nm with low emission for chl *b* region 630-660 nm, so we identify this as a fraction enriched in PSII core dimers. For B8 there is a relative increase in intensity around 630-660nm that we identified as LHCII of PSII SC (Figure 6B). The different fractions were then analyzed by denaturing SDS-PAGE. Except B1 (free pigments and small polypeptides) all fractions contained LHCII polypeptides, LhcbM1-8, (Drop et al., 2014) migrating between 25 and 30 kDa whether the cross-linking agent was present or not (this can be seen by comparing B7- and B7+ in Figure 6C). This shows that GA added to the gradient did not unspecifically cross-link all proteins into complexes, as also observed in the original protocol that was developed to strongly limit intercomplex crosslinking (Stark, 2010). B2+ and B3+ fractions did not contain high MW polypeptides whereas B5+ to B8+ contained large amounts of cross-linked polypeptides in the top part of the gel.

The immunoblot of the SDS-PAGE gel decorated with APE1 antibody in figure 6D shows that all cross-linked bands containing PSII (B5+ to B8+) contained the APE1 polypeptide in the upper part of the gel. B5+ lane showed a specific cross-linking of APE1 with the PSII core and only in the high MW part of the gel while it appeared as a single polypeptide in the non-treated thylakoid samples (Thk). APE1 does not migrate alone or in aggregates when the crosslinker is added showing that when protein-protein interactions are stabilized with GA, APE1 is indeed a PSII protein and not a free protein in the membrane.

PSII is more prone to photoinhibition in *ape1*

Light sensitivity and a decreased maximum quantum efficiency of PSII in high light were observed in *ape1-2* (Figure 1 and Photosynthetic parameters in Supplemental

Table 1), this appeared to be photoinhibition of PSII and defined as destruction of PSII centers occurring at a faster rate than they can be repaired (Adir et al., 2003). To determine whether lower PSII activity in the mutant was due to faster photodamage or due to impaired PSII repair and/or *de novo* synthesis, we applied a photoinhibitory light treatment of 1800 $\mu mol_{photons}.m^{-2}.s^{-1}$ for one hour, with recovery in low light (Figure 7). PSII maximum quantum efficiency and D1 accumulation were monitored (Figure 7A and B). To differentiate between PSII degradation rate and PSII synthesis rate we also performed the experiment in the presence of protein translation inhibitors (lincomycin, LC and chloramphenicol, CAP).

As expected, the presence of translation inhibitors (+LC/CAP) prevented the recovery of F_V/F_M after photoinhibition (1 to 4 hours in Figure 7A). This was due to the block of PSII turnover and D1 synthesis, observed as a decrease in D1 accumulation in the bottom panel of Figure 7B. In the absence of translation inhibitors (-LC/CAP), a smaller decrease in D1 content was observed after an hour (Figure 7B), suggesting that in this instance D1 synthesis partially compensated D1 degradation. The same was also observed on the amplitude of F_V/F_M, consistently greater at 1 hour, showing that PSII was turning over in -LC/CAP conditions (Figure 7A).

The decrease in photosynthetic parameters (Fv/Fm) was paralleled by a decrease in D1, more pronounced in the mutant than in the reference strains (Figure 7B). Since the recovery rate in the mutant was similar to that of the wild type and complemented strain, decrease of D1 in *ape1-2* cells was more due to a faster PSII photoinhibition than a slower PSII repair.

The detoxification enzyme, Glutathionine Peroxidase 5 (GPX5) is a marker for singlet oxygen and PSII dysfunction (Fischer et al., 2009; Roach et al., 2017). GPX5 levels were higher in the mutant already in low light, and its content increased after the photoinhibitory treatment (Figure 7B). This result suggests that a lack of APE1 causes ROS production that elicits a systemic response that we witness by GPX5 accumulation in the mutant, and that the ROS produced is likely to be singlet oxygen issue of PSII.

We next examined the formation of high molecular mass complexes after a high light treatment. We tested different detergent concentrations and found that the dose did

not significantly change the fractionation of complexes which remained stable for each strain (Figure 7C). Notably, the absence or presence of APE1 had a major impact on the pattern of high molecular mass complexes (A-F in Figure 7 and supplemental figure 4). The heaviest band, A, that appears blue and of greater abundance in *ape1-2* is composed of PSII SC, PSI and mitochondrial H^+ATPsynthase (the latter is a contaminant from the thylakoid isolation common in cells grown under these conditions (Rexroth et al., 2003)). The bands B-E are more delineated but less green, suggesting bleaching, compared to the controls. The PSI band, F, is less abundant, suggesting a shift to a higher molecular mass band A in comparison to controls. Importantly, under these conditions, *ape1-2* retains PSII dimeric cores but is lacking the PSII monomeric core and RC47 complexes with an absence of CP43, CP47, D1 and D2 proteins at the expected position in the 2D gel (Supplemental Figure 4).

PSII antenna size, heterogeneity (α- and β-centers) and connectivity between PSII centres

Differences in PSII photoinhibition linked to changes to PSII SC observed in BN-PAGE (Figure 7) led us to test *in vivo* the effective antennae size of PSII in *ape1* under physiological conditions. During a pulse of saturating light Q_A reduction rate is faster than Q_A to Q_B electron transfer and the variable chlorophyll *a* fluorescence increases from F_0 to F_M and is commonly referred to as an OJIP induction. The first phase of this fluorescence rise (OJ phase ~1 ms) reflects PSII antenna size, the faster the rise the larger the functional antenna size (Dinc et al., 2012) (Figure 8). We used a similar treatment as to that shown for the photoinhibition experiment (Figure 7A) and found that *ape1-2* PSII antenna size was slightly increased in comparison to the controls for conditions (i) and (iii) (Table I and Figure 8A). This suggests that *ape1-2* tends towards a larger PSII antenna than both the control lines becoming significantly different after the high light treatment (Table I).

We questioned whether APE1 was affecting the excitonic connectivity of PSII centres, following the method of (Cuni et al., 2004). There were only small differences in the connectivity parameter J between *ape1-2* and WT prior to light treatment (i) (J_{wt} = 3.2±0.3 and $J_{ape1\text{-}2}$ = 4.1±0.5) and after recovery from the light treatment (iii) (J_{wt} = 3.1±0.2 and $J_{ape1\text{-}2}$ = 3.8±0.4). A significant deviation was

observed at the light treatment (ii) in both strains (J_{wt} = 1.4±0.1 and $J_{ape1\text{-}2}$ = 1.5±0.1). This may be due to a smaller fraction of active PSIIs. During photoinhibition, the inactivation of PSII decreases the number of exciton traps as well as the probability of an exciton to hop from center to center. An absence of APE1 did not have an affect on this outcome.

Heterogeneity of PSII antennae was also tested in the presence of DCMU under non-saturating light. Under such conditions, the fluorescence rise is multiphasic. Analysis according to (Melis and Homann, 1976) showed that two phases are observed, one representing the α-centres or large antenna PSII and the other β, or low antenna PSII; no significant differences were observed for conditions (i) but in condition (iii), *ape1-2* had a larger amplitude of the fast phase α (~55%) than the control lines (~42%) suggesting a greater proportion of large antenna PSII SC (Figure 8B).

APE1 changes fractionation profiles of PSII SC during light acclimation

To further characterize the different PSII SC partitioning, *ape1-2* and wild type were grown phototrophically in low and high light at ambient CO_2 in turbidostats. Photosynthetic parameters were monitored (Supplemental table 1). At both light regimes, samples were collected after an acclimated state was reached (around 4 days). Using these conditions, six bands could be identified that contained PSII: PSII SC III, PSII SC II, a band containing PSII and PSI (PSII SC I/PSI), PSII core dimers, PSII core, and RC47 (Figure 9)(labeled in Figure 9A and 9C); and 5 containing PSI (Identified in Supplemental Figure 4).

In low light conditions, in the wild type, PSII was mostly identified as dimeric and monomeric core complexes (Image J relative quantification of D1 from the immunoblot measured: 23% PSII SC; 37% dimeric and 37% monomeric cores; 3% RC47) (Figures 9A and 9C). The *ape1-2* profile was different; PSII SC were more highly represented, observed by D1 signal in the western blot (ImageJ relative quantification of D1 from the immunoblot measured 55% PSII SC; 22% dimeric and 22% monomeric cores; 1% RC47). The PSI profile was also different in *ape1-2*, with a higher abundance of higher molecular mass forms. These features regarding both PSII and PSI confirmed what was observed using milder solubilization.

The high light acclimation treatment (Figure 9B and 9D and silver stained gels in Supplemental Figure 4) resulted in changes to the PSII organization profile in the wild type. The ratio of high to low molecular mass assemblies decreased, where the signal for PSII SC, PSII SC I/PSI and PSII core dimers diminished in favor of PSII core monomers. PSI organization was also changed, with a reduction in the high MW bands. In *ape1-2*, the profile of PSII was less flexible: the same forms of PSII, from RC47 until PSII SC II, were still detectable. This led to a higher ratio of PSII SC to PSII core monomers in the absence of APE1 (Figure 9). Interestingly and despite significant photoinhibtion of *ape1-2*, CO_2 fixation was not affected in comparison to the control strains (Supplemental table I).

Thylakoid structure is altered in *ape1*

Thylakoid membrane structure is determined by a number of factors including photosystem composition, distribution, LHCII interactions and modifications (Kirchhoff, 2019). Interaction of APE1 with PS II, and changes in photosystem oligomeric composition could be linked to modifications at the level of the thylakoid membrane. To verify this, *ape1-2* and wild type cells were grown in phototrophic conditions in low light and ambient CO_2 and the thylakoid membranes were resolved by transmission electron microscopy (Figure 10).

The wild type appeared to have more organized thylakoid membranes as opposed to *ape1-2*, where thylakoids showed disorganized or uneven margins (Figures 10A and B and Supplemental Figure 5). Quantitative analysis (Figure 10C) showed that the mutant thylakoid stacks had more layers, often more than 7; against 3 - 4 on average in the wild type (Figure 10D). *ape1-2* stacks were shorter, always less than 1 µm, while the wild type showed membranes appressed over > 1 µm (Figure 10E). Statistical analysis showed that the differences observed were significant.

Calculation using the parameters found in Figure 10C and in (Engel et al., 2015) showed that the *ape1-2* mutant shows a 50% increase in the ratio of grana height to diameter compared to the wild type, and a 40% increase in the area of appressed to unappressed membranes (Supplemental Table 2). This is due to a larger stacked area and to a decreased end membrane surface, even though the area of the margins is about 20% higher in the mutant.

Differential solubilization of thylakoids of the wild type and *ape1-2* was performed to correlate changes in thylakoid structure with the localization of the photosystems (Figures 10F and 10G). We used digitonin to preferentially solubilize end membranes/stroma lamellae of thylakoids and then solubilized the remaining pellet (assumedly mostly stacked regions/grana) with β-DM and these were separated by BN PAGE (4-16%). We observed a lower yield on a per chlorophyll basis for digitonin solubilization in *ape1-2*, suggesting less LHCII (red arrow) and a reduction in low molecular mass PSII (black arrow), expected to accumulate preferentially in the end membranes and stromal lamellae regions as seen in the wild type (Figure 10F). The subsequent treatment of *ape1-2* with β-DM showed enrichment in high molecular mass oligomeric forms of PSII (black arrows), in the more stacked regions of the membranes (Figure 10G).

Discussion

Structure and function of the photosystems and their arrangement in the thylakoid membrane are constantly adjusting to changes in their environment allowing them to maintain performance and to cope with stress. Modulating PS II oligomeric composition and antenna size in response to high light is a key parameter for light acclimation. The sum of acclimation mechanisms that an organism has at its disposal contributes to the fitness of a species and understanding these is fundamental to our comprehension of ecology and evolution, and to the future improvement of CO_2 capture and utilization by photosynthetic organisms.

Proteomic studies in Chlamydmonas (Terashima et al., 2011), maize (Majeran et al., 2008) and Arabidopsis (Myouga et al., 2018; Tomizioli et al., 2014) have listed APE1 amongst the peptides found in thylakoid membranes. Western blot analysis on fractionated chloroplasts demonstrated that APE1 is an integral membrane protein, bound to the thylakoids (Figure 2). APE1 belongs to the GreenCut, the pool of gene models conserved across plants and green algae and this protein is absent from non-photosynthetic organisms (Merchant et al., 2007). More specifically, APE1 is part of the ‘PlastidCut + cyanobacteria’ (Heinnickel and Grossman, 2013). Comparative genomics of cyanobacteria showed that APE1 is part of their core genome, encompassing only 63 gene models shared with all oxygenic photosynthetic organisms (Mulkidjanian et al., 2006). The other conserved regulatory proteins in this

group include GUN4 and THF1. A more recent analysis (Beck et al., 2018) compared the genome of 77 cyanobacterial species including the oceanic nitrogen-fixing cyanobacterium UCYN-A and *cyanobacterium endosymbiont of Epithemia turgida EtS* that have lost PSII and the genes for carbon fixation (Zehr et al., 2008). From the cross analysis of these different data sets we identified co-occurrence of APE1 with 7 PSII core subunits, that is, at the origins of oxygenic photosynthesis (Supplemental Table 3). This very early conservation may suggest that we have identified APE1 in the regulatory role that permits PSII heterogeneity and increases fitness and flexibility of the photosynthetic apparatus across all oxygenic photosynthetic species. However, the *ape1* phenotype is only observed under high light that suggests it became less important during evolution, as the repertoire of PSII repair and regulatory pathways has expanded over time. Rather than being a sole regulator it is probably now integral to a set of pathways involved in light acclimation (such proteins as CURT and STT7/8 could be considered to fall within the same category) that together optimize thylakoid structures in line with light conditions (Pribil et al., 2014; Pribil et al., 2018).

Chlamydomonas *ape1* mutants show an increased light sensitivity compared to WT, due to the ROS formation as indicated by increase in GPX5 (Figure 7, (Fischer et al., 2009; Roach et al., 2017)). The increase in ROS, more specifically $^1O_2$, results from destabilized PSII/impaired acclimation but this phenotype is alleviated under high CO_2 conditions (Figure 1). It appears as a common trait that when a regulatory pathway is missing, affecting either light-harvesting, electron transport or CO_2 capture, that growth is retarded under restrictive conditions (rather high light >300 $\mu mol_{photons}.m^{-2}.s^{-1}$, limiting CO_2) while more permissive conditions (either moderate light <100 $\mu mol_{photons}.m^{-2}.s^{-1}$ or high CO_2) restore normal growth. Other defects in regulation of photosynthesis have similar consequences on phototrophic growth: *pgr5* in *C. reinhardtii* and *Arabidopsis* (Johnson et al., 2014; Munekage et al., 2008), *pgrl1* (Dang et al., 2014), *cas* (Wang et al., 2016), *psbS* (Correa-Galvis et al., 2016b), *npq4* (Chaux et al., 2017), as well as 1 in 5 mutants annotated as *acetate requiring* in (Dent et al., 2005). Under limiting CO_2, linear electron flow is limited at the PSI acceptor-side and in green algae O_2 is also used as an alternative electron acceptor to relieve acute reduction of electron carriers through the Flv Pathway (Chaux et al., 2015) or through the shuttle of reduced metabolites to the

mitochondrion for oxidative phosphorylation (Dang et al., 2014; Larosa et al., 2018). Whereas O_2 photoreduction mostly damages PSI as observed in mutants impaired for cyclic electron flow (Johnson et al., 2014), an absence of APE1 results in PSII photodamage (Figure 1, 7 and Supplemental table 1).

The biophysical assay of antenna size, α- and β-centers and connectivity (Figure 8) confirmed that despite changes to supramolecular membrane organization that affect effective antenna size, the functional interaction between PSII units (the connectivity experiment to measure excitonic coupling) were not affected between *ape1* and the wild type. This suggests again for APE1 a regulatory role rather than at the level of the PSII function. Similarly, APE1 is not required for PSII biogenesis (Figure 3). Neither did we find it to be directly involved in PSII repair or *de novo* synthesis (Figure 7). Instead, an accelerated degradation of D1 protein as well as an increased accumulation of GPX5 were observed in *ape1* (Figure 7) and both these effects are linked to singlet oxygen production at the level of PSII. PSII photoinhibition increases linearly with light intensity (Tyystjarvi and Aro, 1996) and ROS production in isolated thylakoids in vitro is dependent on membrane stacking (Khatoon et al., 2009). Thus, the light sensitivity and PSII photoinhibition observed in *ape1* is correlated to the retention of PSII SC and the greater number of appressed membranes (Figure 7C and 10). The *ape1* mutant has a reduction in PSII core monomers and RC47 when grown photrophically in low light (Figure 4) more likely due to the remodeling of PSII cores into SC and not simply due to a deficient PSII repair cycle. However, as PSII heterogeneity is important for repair, it is clear that there is some overlap between these two processes. The lack of coordination between PSII core and antenna under non-stressful conditions, that results in suboptimal accumulation of PSII core proteins, D1 and D2 (-20%) and an increase in total LHCII antenna (+20%) (Figure 3) suggests that APE1 has a constitutive function in maintenance of PSII, in line with a regulatory role in light acclimation.

When PSII is photodamaged, D1 requires repair and the first step is the disassembly of PSII SC to core monomers followed by unfolding of thylakoid membranes (Lu, 2016; Theis and Schroda, 2016). Psb29 / Thylakoid Formation 1 (THF1) is involved in this disassembly process via interaction with the FtsH protease and LHCII antenna

(Bec Kova et al., 2017; Huang et al., 2013). In our model, APE1 responds to an increase in light by releasing the oligomeric structure of PSII SC, prior to the disassembly of PSII megacomplexes by THF1 and FtsH protease for PSII repair illustrated by the model (Figure 11). APE1 binds to PSII core and not LHCII, perhaps preferentially accumulated in stromal lamellae and margins of stacked regions as measured in (Tomizioli et al., 2014). When in PSII SC, it releases core complexes as dimers and monomers. As a consequence, PSII heterogeneity influences the stacking of Chlamydomonas thylakoids, promoting longer and less stacked membranes with an increased volume of end membranes.

Worth commenting on is the effect on PSI complexes observed in *ape1-2* (Figures 4,7 and 9). After ruling out an interaction with PSI (Figure 5) we propose that the more compact and more stacked membranes in *ape1-2* compared to the wild type likely result in greater stability and fractionation of the higher molecular mass PSI-LHCA complexes. This was similarly observed in the *PsbN* mutant, a *bona fide* PSII repair protein, with as a consequence disrupted thylakoids, that accumulates higher order PSI complexes (Torabi et al., 2014).

During high light acclimation in plants, it takes up to 2 days for the antenna proteins to be degraded. Yang and co-workers (Yang et al., 1998) found that none of the known chloroplast proteases were involved in this process. This suggests the existence of a new unknown process in the degradation of antennae that could be autophagy. In a study of ATl1t (Autophagy-related 8 interacting protein 1) using split ubiquitin and BiFC assays (Michaeli et al., 2014), ATL1 was shown to interact with 13 chloroplast proteins including APE1 and PsbS. The exact interpretation of this result is unclear, but it could suggest that photoprotection proteins, which are necessary under stress conditions, are resistant to proteases and are only targeted for degradation under conditions where cell death is impending. It could also point to a more complex role for APE1 and PsbS as markers for selective high light acclimation as vesicle cargo for plastid remodeling (Baena-Gonzalez and Sheen, 2008; Khan et al., 2013).

Very few specific regulators have been directly attributed to the light acclimation process since it was first described in Björkman's pioneering work (Björkman and Ludlow, 1972). Photosystem and antenna remodeling in response to light intensity characterized there and in later studies (Anderson et al., 1988; Melis, 1991) is coherent with what is witnessed in the *ape1* mutant phenotype of both Chlamydomonas and Arabidopsis (Walters et al., 2003). We envisage two possibilities for a mode of action: (1) Via an interaction with the PSII core, APE1 may destabilize the density packing of thylakoids by impairing hydrophobic interactions between transmembrane helices. (2) APE1 contains a soluble domain, with highly conserved charged residues (Glu, Asp, Arg, His) (shown in Supplementary Figure 2) which may bind, release or sense a substrate that changes electrostatic or Van der Waals attraction between polypeptides across the stromal gap. We predict that APE1 may only be involved in a very initial stage of the light acclimation process whereby it responds to light by enabling PSII SC to disassemble promoting PSII core complex heterogeneity and thylakoid destacking. Only under high light conditions, in Chlamydomonas, does this process become critical for survival.

Materials and Methods

Strains. The wild type strain (Jex4 *mt*$^{-}$) used in this study is a progeny of 137c backcrosses. *ΔrbcL 2A mt*$^{-}$ strain used as the recipient strain for generation of the mutant library comes from a backcross of *ΔrbcL* strain (Johnson et al., 2010) and described as the "control" strain in figure 1. *ΔrbcL 2A mt-* strain was transformed with the *aphVIII* cassette obtained by digestion with SacI and KpnI of the pBC1 plasmid derived from pSI103 (Sizova et al., 2001). Cells were plated on TAP containing 15 µg.mL^{-1} Paromomycin. *ape1-1* strain is the progeny of *ΔrbcL ape1* obtained in the generated mutant library, outcrossed to Jex4 *mt+* twice. *ape1-2* strain is the progeny of two outcrosses of strain LMJ.RY0402.039504 from CliP (Li et al., 2016) with Jex4 *mt*$^{+}$ and *mt*$^{-}$. Complemented strains were generated as described in "Transformation" using the vector obtained as described in "vector construction for nuclear complementation" below. *psbA* and *psaB* are the Fud7 and C3 mutants, a gift from F.A. Wollman.

Cell culture. Cell cultures were grown in Tris-Acetate-Phosphate medium at 25°C under ambient air at 10 $\mu mol_{photons}.m^{-2}\ s^{-1}$ in incubation shakers, this is referred to as heterotrophic conditions in the text, and when stated, shifted to phototrophic conditions by centrifugation and resuspension in minimal media under ambient air. Cells were always kept at exponential phase by daily dilution to a density of around $1\text{-}2.10^6$ cells.mL^{-1}. Experiments performed using batch culture were done in 250 or 500 mL Erlenmeyer flasks. Standard recipes were used as in (Harris, 1989). Maintained cultures were always cultivated at < 10 $\mu mol_{photons}.m^{-2}\ s^{-1}$ in solid TAP media.

Turbidostats. Photobioreactors were run as turbidostats (OD_{880} maintained at 0.4 by addition of fresh minimal medium). Set-up was the same as in (Chaux et al., 2017), except that the CO_2 input was maintained constant at ambient level (correction to avoid natural daily CO_2 variation). Light conditions used were 40 and 320 $\mu mol_{photons}.m^{-2}.s^{-1}$. Samples were taken by pressurizing the culture tank, for microscopy analysis, BN-PAGE, pigment content, and photosynthetic parameters. Wild type and *ape1-2* cells were grown in triplicates in photobioreactors in low light until their growth in these conditions stabilized, we called this an “acclimated state”. We took samples of these cultures for detailed biochemical analysis. Cells that had reached an acclimated state at low light were then subjected to high light, saturating for photosynthesis. Again, we allowed the growth rates of the cells to stabilize (about 5 days) before sampling the cultures.

DNA extraction. DNA extraction was performed either according to a phenol-chloroform method or according to a rapid total DNA extraction with Chelex 100 (Sigma).

RESDA-PCR adapted from (Gonzalez-Ballester et al., 2005). First amplification was done in 20 µL with DegPstI (degenerated primers) and Rb1 (on the *aphVIII* cassette) primers with Taq polymerase (NEB) using 58°C annealing temperature for 5 cycles, *25°C and then 55°C for 1 cycle, 58°C for 2 cycles, 40°C for 1 cycle*, repeated 20 times between *. The PCR mix was then diluted 1000 times and 1 µL used as matrix for the second amplification. The latter was done using KOD Xtreme polymerase (Novagen) with Q0 (on an adaptator on DegPstI primer) and Rb4 (on the cassette),

using 60°C annealing temperature for 32 cycles. Fragments were loaded on 1% agarose gels, the band of interest excised from the gel and cleaned using Macherey-Nagel™ NucleoSpin™ Gel and PCR Clean-up Kit and cloned into pGEM-T (Promega) for amplification before sequencing.

Genome mapping. *ΔrbcL ape1* full insertion site in *APE1* was amplified from phenol-chloroform extracted DNA using primer A (5'- CATAACCCAGACCCCCAGAG-3') and B (5'-CAGACTCATCCGGACCCCAA-3') on genomic DNA, from either side of the insertion, using LA-Taq (Thermo Scientific, 60°C, 30 cycles). LMJ.RY0402.039504 was subcloned, and DNA extracted using the Chelex 100 method. The 3' side of the insertion was amplified using primer D (5'-GACGTTACAGCACACCCTTG-3') on the cassette and C (5'-ATCTCTTTCGGGTCCATCCT-3') primer 600 bp upstream on genomic DNA (LA-Taq, 60°C, 30 cycles).

RT-PCR. Cells were grown in TAP low light conditions. RNA was isolated using the PureLink RNA reagent from Invitrogen according to the manufacturer instructions, treated by TURBO DNAse enzyme (Applied Biosystems) and purified with NucleoSpin RNA Clean-up kit (Macherey-Nagel). RNA was quantified by Nanodrop (Thermoscientific). cDNA was synthesised using the standard SuperScript III protocol (Invitrogen) with oligo-dT primers. cDNA was amplified by PCR using the housekeeping gene, *RAK* as positive control and using primers E (5'-ACCTATCCTCGCTGTTCCTG-3') and F (5'-CACGTCCTTCTTGTCCTTGC-3') for *APE1* for 30 cycles.

Genetic transformation. 300 µL of cell culture resuspended at around 1-2.10^8 cells.mL^{-1} in TAP 60 mM Sucrose were aliquoted in 0.4 cm gapped cuvettes. 1 µg of linearized DNA and 4 µL of salmon sperm DNA were added and cells were incubated 20 min on ice. Negative controls were done without adding DNA. Electroporation conditions were 1000 V, 25 µF. Cells were allowed to recover in low light overnight in 10 mL TAP 60 mM Sucrose, centrifuged and resuspended in 500 µL TAP. Volumes from 50 µL to 200 µL were plated on TAP containing antibiotics to obtain an optimal colony density. The *ape1-2* mutant was transformed with a plasmid containing Zeo^R cassette and the genomic version of the wild type *APE1* under its native promoter

(1500 bp upstream of the start site of *APE1*). Transformants were selected on zeocin-containing plates and were screened using chlorophyll fluorescence imaging

Vector construction for nuclear complementation. Transformation plasmid was constructed using restriction site cloning in pMS188 (Schroda et al., 2002) containing a bleomycin resistance cassette. *APE1* gene with an additional 1500 bp on the 5' side and 500 bp on the 3' side was amplified by PCR using Q5 High-Fidelity DNA Polymerase (NEB) using primers 5'-TTATAATACCCACCCGTCAAAGCTGTG-3' and 5'-TTATAACAGACTCATCCGGACCCCAA-3' containing an additional PsiI restriction site (70°C, 30 cycles). pMS188 was digested using PsiI and dephosphorylated. Ligation was done in 20 µL overnight at 4°C using 50 ng of pMS188 and 140 ng of the purified PCR product. DH5-α bacterial strains were transformed and plated on plates containing Kanamycin. Presence and orientation of *APE1* gene in pMS188 was then checked by digestion using XbaI, yielding 3 fragments of 1.6, 2.9 and 4.5 kb on 1% agarose gel. The construct was then verified by sequencing using 5'-TACCCACCCGTCAAAGCTGTG-3', 5'-GGCGTCTTCCACACTCACTG-3', 5'-CACACCACTCCCGTAGCTGA-3', 5'-GAGGTGATCGCTTCGGTAGG-3' and 5'-TGGACGCAAATGGAAACAAG-3' primers. The transformation plasmid was then linearized with ScaI-HF, transformation was done as stated above, and cells were plated on TAP containing Zeocin at 45 µg.mL^{-1}.

Recombinant APE1 protein production. *APE1* cDNA without the sequence coding for the transit peptide (APE1 total protein, 223 amino acids) or without the sequence coding for the transmembrane domain (APE1 soluble region, 156 amino acids) was introduced in pLIC03 vector (LIC : ligation-independent cloning; (Aslanidis and de Jong, 1990) using GoldenGate cloning technique. The pLIC03 vector is the pET-28a+ vector (Novagen) modified to add downstream of the start codon a 6×His tag and a TEV protease-cleavage site. These are followed by the suicide gene *sacB* flanked by *BsaI* restriction sites, replaced by *APE1* cDNA flanked by complementary *BsaI* restriction sites sequences. 50 ng of vector was used with 1:3 cDNA for six successive rounds of digestion (*BsaI*, 37°C, 5 min) and ligation (T4 ligase, 16°C, 10 min) in the same mix. Successful ligation of *APE1* cDNA removes the *BsaI* recognition sequence. The cycles were ended by a final ligation step (30 min at 16°C). DH5□ *E. coli* cells were then transformed with the ligation products for vector

687 amplification, screening and sequencing. 65 ng of vectors were then used to
688 transform Rosetta *E. coli* cells cultured in TB medium at 37 °C up to OD 1. IPTG was
689 added to induce APE1 recombinant protein expression, temperature was decreased
690 to 17 °C and the cells were grown for an additional 18 h. Cells were harvested by
691 centrifugation and the pellet was resuspended in lysis buffer during 30 min at 4°C.
692 Lysis buffer contained 300 mM NaCl, 50 mM Tris pH 8.0, 10 mM imidazole, 5% (w/v)
693 glycerol, 0.25 $mg.mL^{-1}$ lysozyme, 0.1% Triton, 1mM EDTA and protease inhibitors.
694 Cells were lysed by sonication, and incubated at 25°C with 20 mM $MgSO_4$ and 10
695 $\mu g.mL^{-1}$ DNase. The lysate was then centrifuged; the supernatant was collected and
696 incubated for 5 min on 1 mL Ni Sepharose® 6Fast Flow (GE Healthcare) equilibrated
697 with 10 mL binding buffer. The resin was washed (5 x 1mL) and eluted (5 x 1mL).
698 Buffers contained 300 mM NaCl, 50 mM Tris pH 8.0, 5% (w/v) glycerol; with 10 mM
699 imidazole for binding, 50 mM for washing and 250 mM for elution.
700
701 **Antibody generation.** APE1 recombinant protein containing only the soluble part
702 was sent to ProteoGenix for antibody production from rabbit. 9 mL of filtered immune
703 serum were purified against the soluble part of the recombinant protein (10 mg)
704 covalently coupled to 1mL HiTrap NHS-activated HP resin (GE Healthcare) according
705 to the manufacturer instructions. The serum recirculated on the resin for 2 hours at a
706 flow rate of 0.5 mL/min and was eluted at pH 3. The eluted fraction was collected in
707 neutralizing buffer. The antibody is used at 1:10000 dilution for immunoblotting.
708
709 **Spot tests.** 25µL of cells at 10^6 $cells.mL^{-1}$ were spotted on TAP or MIN plates,
710 allowed to dry and placed at different light intensities as shown for 5-14 days.
711
712 **Pigment quantification.** Chlorophyll content was measured in acetone 80%
713 according to Porra et al. (1989) or in methanol using:
714 $Chlorophyll\ a = 15{,}65 \cdot (OD_{666} - OD_{750}) - 7{,}34 \cdot (OD_{653} - OD_{750})$
715 $Chlorophyll\ b = 27{,}05 \cdot (OD_{653} - OD_{750}) - 11{,}21 \cdot (OD_{666} - OD_{750})$
716 $Carotenoids\ (X + C) = (1000 \cdot (OD_{470} - OD_{750}) - 2.86 \cdot Chl\ a - 129.2 \cdot Chl\ b) / 221$
717
718 **Protein Analysis.** Proteins were extracted from total cells or thylakoids with cold
719 acetone 80% and separated under denaturing conditions on 13% SDS-PAGE gels,
720 unless otherwise indicated. Proteins were loaded based on chlorophyll content (1

721 µg), and total protein amount was quantified on Coomassie Blue gels to adjust the
722 loading. SYPRO Ruby Protein gel stain was performed according to manufacturers
723 protocol (Molecular Probes, Invitrogen). Proteins were transferred onto nitrocellulose
724 membranes (BioTrace NT, Pall Corporation) using liquid transfer (except for Figure
725 4D where 10% NativePAGE Bis-Tris MES gel (Invitrogen) and a semi-dry transfer
726 was performed. All primary antibodies used were sourced from Agrisera. APE1
727 antibody was generated in a rabbit against the soluble part of the recombinant
728 protein. Secondary antibodies used were always HRP-conjugated anti-rabbit
729 (Invitrogen). HRP-peroxidase chemiluminescent substrate (Invitrogen) was used to
730 reveal the antibody signal using the GBOX imaging system (Syngene).
731
732 **Thylakoid extraction and native protein analysis.** Thylakoid extraction was done
733 according to the standard method (Chua and Bennoun, 1975). Thylakoids were
734 resuspended in Hepes 5 mM, EDTA 10 mM at 1 mg/mL chlorophyll for subsequent
735 SDS-PAGE analysis. For density gradient analysis and crosslinking, 1% digitonin
736 (final) and then 1% n-Dodecyl- α -D-Maltoside (final) with 0.35% glutaraldhyde was
737 loaded onto sucrose gradients and treated as in (Caffari et al.,ref). For non-
738 denaturing conditions, thylakoids were resuspended in NativePAGE sample buffer
739 (Life technologies) at 1 mg.mL-1 chlorophyll, thylakoids were solubilized for 5 min on
740 ice in the same volume of 2% n-Dodecyl-β-D-Maltoside (0.5 mg.mL-1 chlorophyll and
741 1% n-Dodecyl-β-D-Maltoside final). Differential solubilization was achieved by using
742 1% digitonin (final) and then 1% n-Dodecyl-β-D-Maltoside (final) on the remaining
743 non-solubilized material. For interaction analysis, thylakoids were solubilized with
744 0.5% digitonin (final) and 0.5% n-Dodecyl-α-D-Maltoside (final). Concentrations and
745 resulting profiles were similar to that observed in (Pagliano et al., 2012) and were
746 confirmed in figure 6. For each analysis, 20 µL were then loaded with 2 µL of G-250
747 sample additive (Life technologies) on 4-16% (Figures 4A and 7) or 3-12% (figures
748 4C and 6) NativePAGE gels (Life technologies). Cathode Running buffer (Life
749 technologies) was supplemented with 0.02% G-250 for 2/3 of the migration, and with
750 0.002% G-250 for the remaining third. For second dimension analysis, bands were
751 incubated 1h at room temperature in LDS, 50 mM DTT and 5 M Urea and loaded on
752 13% 5M urea SDS-PAGE. Gels were then either transferred on nitrocellulose or
753 silver stained. Proteins separated by BN-PAGE were identified using immunoblots
754 and silver staining on the second dimension, and by comparison to similar results in

the literature (Drop et al., 2011; Drop et al., 2014; Muranaka et al., 2016; Rexroth et al., 2003). Spectra of gradient fractions (350 -750 nm) were obtained using UV-Vis spectrophotometer (Varian Cary 300) at a scan rate of 240 nm/min and baseline correction.

Chlorophyll Fluorescence Analysis

Fluorescence measurements on Petri dishes were performed using the set up for *in vivo* chlorophyll fluorescence imaging (Beal SpeedZen Camera) (Johnson et al., 2009). Pulse-Amplitude-Modulation Fluorimeter (Walz) was used for chlorophyll fluorescence kinetics and monitoring of photoinhibition. Dark-adapted cells were subjected to a saturating pulse (8 000 $\mu mol_{photons}.m^{-2}.s^{-1}$) to measure F_V/F_M or exposed to a given light intensity (red light) and Φ_{PSII} was probed every minute. Using the saturating pulse but with fast sampling kinetics, OJIP was monitored over 300 milliseconds. Heterogeneity of PSII centres and connectivity of PSII centres was performed using the Joliot-type Spectrophotometer (JTS-Biologic). Melis has shown that the complementary area over the fluorescence curve (proportional to the reduction of Q_A) of DCMU poisoned sample shows two phases in a semi-logarithmic plot (Melis and Homann, 1976). The fast phase, or α-centers, appearing as a straight line at $0 < t < 50$ ms corresponds to PSII with a large light harvesting capacity, whereas the slow phase, or β-centers, visible between $100 < t < 250$ ms corresponds to PSII centers with less associated chlorophylls (core complex). The intercept of the slow component at $t = 0$ (dotted lines) allows for quantification of the α-centers. Connectivity was performed as in (Cuni et al., 2004) 10 µM DCMU was used to block electron transfer beyond Q_A. Connectivity between PSII centers is illustrated by the non-linearity between the variable part of chlorophyll fluorescence yield (probability to reemit a photon) against the relative concentration of reduced Q_A and data were fitted to $F_V = [Q_A^-] / (1 + J - J [Q_A^-])$ yielding the connectivity parameter J.

Photoinhibition experiments. Cells were grown in TAP media at 10 $\mu mol_{photons}.m^{-2}.s^{-1}$, diluted to a similar chlorophyll amount (3 $\mu g.mL^{-1}$), allowed to stabilise for 1 hour at 40 $\mu mol_{photons}.m^{-2}.s^{-1}$, and then transferred to 1800 $\mu mol_{photons}.m^{-2}.s^{-1}$ light for 1 hour with or without 0.1 mg/mL chloramphenicol and 0.5 mg/mL lincomycin. Recovery was done at 40 $\mu mol_{photons}.m^{-2}.s^{-1}$. F_V/F_M was used as a non-invasive

789 measure of the maximum PSII quantum efficiency to monitor the degree of
790 photoinhibition caused by the light treatment. Cells were placed in the dark for 3
791 minutes with agitation before the measurement by PAM.
792
793 **Electronic Transmission Microscopy.** This experiment was performed twice on two
794 different sets of cultures: cells were grown phototrophically and samples were taken
795 either from turbidostats grown at 40 $\mu mol_{photons}.m^{-2}.s^{-1}$ or from batch culture flasks
796 grown at 80 $\mu mol_{photons}.m^{-2}.s^{-1}$ (statistics are a mix of both samples). Cells were
797 collected by centrifugation and fixed with 2.5% glutaraldehyde in 0.1 M sodium
798 cacodylate buffer, pH 7.4, at 4 °C for two days. They were then washed three times
799 using the same buffer. Samples were post-osmicated with 1% osmium tetroxyde in
800 cacodylate buffer for 1 h, dehydrated through a graded ethanol series, and finally
801 embedded in monomeric resin Epon 812. All chemicals used for histological
802 preparation were purchased from Electron Microscopy Sciences (Hatfield, USA). 90
803 nm ultrathin sections for transmission electron microscope (TEM) were obtained by
804 an ultramicrotome UCT (Leica Microsystems GmbH, Wetzlar, Germany) and
805 mounted on copper grids. They were examined in a Tecnai G^2 Biotwin Electron
806 Microscope (ThermoFisher Scientific FEI, Eindhoven, the Netherlands) using an
807 accelerating voltage of 100 kV and equipped with a CCD camera Megaview III
808 (Olympus Soft imaging Solutions GmbH, Münster, Germany). For each replicate,
809 several photographs of entire cells and at least 20 micrographs of local detailed
810 structures were taken, analyzed and compared.
811
812 **Accession numbers**
813 Sequence data for *C. reinhardtii APE1* from this article can be found in GenBank
814 under the accession number NW_001843882.1.
815
816 **Supplementary dMaterial files**
817 **Fig S1.** Mapping of the insertion in the *APE1* gene of Chlamydomonas in two alleles.
818 **Fig S2.** Summary scheme of highly conserved domains in APE1: Alignments of
819 predicted protein sequences for *APE1* gene products.
820 **Fig S3.** Silver stain of 2nd dimension BN-PAGE of thylakoid proteins of *ape1-2* , *psbA*
821 and *psaB* cells treated by high light in batch cultures.

Fig S4. Silver stain of 2nd dimension BN-PAGE thylakoid proteins of WT and *ape1-2* acclimated to high light in photobioreactors run as turbidostats.

Fig S5. TEM images at two different magnifications of thylakoid membranes from wild type and *ape1-2*.

Table S1. Photosynthetic parameters in different conditions

Table S2. Dimensions and membrane surfaces of the grana (stacked regions) in WT and *ape1-2* cells.

Table S3. List of cyanobacterial proteins conserved across all oxygenic phototrophs having the same genomic co-occurrence as APE1

	condition (i) Low light			condition (iii) Low light acclimated after high light		
	WT	*ape1-2*	*ape1-2:*APE1	WT	*ape1-2*	*ape1-2:*APE1
F $t_{1/2}$ (ms)	0.199±0.017	0.171±0.013	0.189±0.011	0.214±0.018	0.175±0.005*	0.225±0.009

Table I. Fluorescence half rise times are shown for *ape1-2* and control lines before the light treatment, (i) and after (iii) using mean values (n=3) with SEM. * denotes that *ape1-2* was $p < 0.05$ significantly different from the controls.

Acknowledgements

We would like to thank Jerome Lavergne for invigorating and informative discussions and Corinne Cassier-Chauvat for help on cyanobacterial genome analysis. We acknowledge and are thankful to Stéphanie Blangy, Audrey Beyly-Adriano, Pascaline Auroy and Véronique Cardettini for technical assistance. This work was supported by a grant from the Agence National pour la Recherche (ChloroPaths : ANR-14-CE05-0041-01). M.C. was supported by a scholarship from the Ministery of Science and Education.

Author Contributions

MC, JA, JD, MF, GP, BG, XJ designed the research; MC, JA, SC, PB, SC, JD, MF, XJ performed research; MC, JA, SC, PB, SC, JD, MF, GP, BG, XJ analyzed data; and MC, JA, SC, XJ wrote the paper.

References

Adir, N., Zer, H., Shochat, S., and Ohad, I. (2003). Photoinhibition - a historical perspective. Photosynthesis research *76*, 343-370.

Albanese, P., Melero, R., Engel, B.D., Grinzato, A., Berto, P., Manfredi, M., Chiodoni, A., Vargas, J., Sorzano, C.O.S., Marengo, E., *et al.* (2017). Pea PSII-LHCII supercomplexes form pairs by making connections across the stromal gap. Scientific reports *7*, 10067.

Albanese, P., Nield, J., Tabares, J.A., Chiodoni, A., Manfredi, M., Gosetti, F., Marengo, E., Saracco, G., Barber, J., and Pagliano, C. (2016). Isolation of novel PSII-LHCII megacomplexes from pea plants characterized by a combination of proteomics and electron microscopy. Photosynthesis research *130*, 19-31.

Anderson, J.M., Chow, W.S., and Goodchild, D.J. (1988). Thylakoid membrane organisation in sun/shade acclimation. . Austr J Plant Physiol *15*, 11–26.

Anderson, J.M., Chow, W.S., and Park, Y.I. (1995). The grand design of photosynthesis: Acclimation of the photosynthetic apparatus to environmental cues. Photosynthesis research *46*, 129-139.

Aslanidis, C., and de Jong, P.J. (1990). Ligation-independent cloning of PCR products (LIC-PCR). Nucleic acids research *18*, 6069-6074.

Baena-Gonzalez, E., and Sheen, J. (2008). Convergent energy and stress signaling. Trends in plant science *13*, 474-482.

Bec Kova, M., Yu, J., Krynicka, V., Kozlo, A., Shao, S., Konik, P., Komenda, J., Murray, J.W., and Nixon, P.J. (2017). Structure of Psb29/Thf1 and its association with the FtsH protease complex involved in photosystem II repair in cyanobacteria. Philosophical transactions of the Royal Society of London Series B, Biological sciences *372*.

Beck, C., Knoop, H., and Steuer, R. (2018). Modules of co-occurrence in the cyanobacterial pan-genome reveal functional associations between groups of ortholog genes. PLoS genetics *14*, e1007239.

Bielczynski, L.W., Schansker, G., and Croce, R. (2016). Effect of Light Acclimation on the Organization of Photosystem II Super- and Sub-Complexes in Arabidopsis thaliana. Frontiers in plant science *7*, 105.

Björkman, O., and Ludlow, M.M. (1972). Characterization of the light climate on the floor of a Queensland rainforest. . Carnegie Inst Washington Yearbook *71*, 85–94.

Boekema, E.J., van Breemen, J.F., van Roon, H., and Dekker, J.P. (2000). Arrangement of photosystem II supercomplexes in crystalline macrodomains within the thylakoid membrane of green plant chloroplasts. Journal of molecular biology *301*, 1123-1133.

Boekema, E.J., van Roon, H., Calkoen, F., Bassi, R., and Dekker, J.P. (1999). Multiple types of association of photosystem II and its light-harvesting antenna in partially solubilized photosystem II membranes. Biochemistry *38*, 2233-2239.

892 Bricker, T.M., and Ghanotakis, D.F. (1996). ntroduction to Oxygen Evolution and the
893 Oxygen-Evolving Complex. In Oxygenic Photosynthesis: The Light Reactions
894 Advances in Photosynthesis and Respiration O. D.R., Y. C.F., and H. I.F., eds.
895 (Dordrecht: Springer).
896 Caffarri, S., Kouril, R., Kereiche, S., Boekema, E.J., and Croce, R. (2009). Functional
897 architecture of higher plant photosystem II supercomplexes. The EMBO journal *28*,
898 3052-3063.
899 Caffarri, S., Tibiletti, T., Jennings, R.C., and Santabarbara, S. (2014). A comparison
900 between plant photosystem I and photosystem II architecture and functioning.
901 Current protein & peptide science *15*, 296-331.
902 Chaux, F., Johnson, X., Auroy, P., Beyly-Adriano, A., Te, I., Cuine, S., and Peltier, G.
903 (2017). PGRL1 and LHCSR3 Compensate for Each Other in Controlling
904 Photosynthesis and Avoiding Photosystem I Photoinhibition during High Light
905 Acclimation of Chlamydomonas Cells. Molecular plant *10*, 216-218.
906 Chaux, F., Peltier, G., and Johnson, X. (2015). A security network in PSI
907 photoprotection: regulation of photosynthetic control, NPQ and O2 photoreduction by
908 cyclic electron flow. Frontiers in plant science *6*, 875.
909 Choquet, Y., Wostrikoff, K., Rimbault, B., Zito, F., Girard-Bascou, J., Drapier, D., and
910 Wollman, F.A. (2001). Assembly-controlled regulation of chloroplast gene translation.
911 Biochemical Society transactions *29*, 421-426.
912 Chua, N.H., and Bennoun, P. (1975). Thylakoid membrane polypeptides of
913 Chlamydomonas reinhardtii: wild-type and mutant strains deficient in photosystem II
914 reaction center. Proceedings of the National Academy of Sciences of the United
915 States of America *72*, 2175-2179.
916 Correa-Galvis, V., Poschmann, G., Melzer, M., Stuhler, K., and Jahns, P. (2016a).
917 PsbS interactions involved in the activation of energy dissipation in Arabidopsis.
918 Nature plants *2*, 15225.
919 Correa-Galvis, V., Redekop, P., Guan, K., Griess, A., Truong, T.B., Wakao, S., Niyogi,
920 K.K., and Jahns, P. (2016b). Photosystem II Subunit PsbS Is Involved in the Induction
921 of LHCSR Protein-dependent Energy Dissipation in Chlamydomonas reinhardtii. The
922 Journal of biological chemistry *291*, 17478-17487.
923 Cuni, A., Xiong, L., Sayre, R., Rappaport, F., and Lavergne, J. (2004). Modification of
924 the pheophytin midpoint potential in photosystem II: Modulation of the quantum yield
925 of charge separation and of charge recombination pathways. Physical Chemistry
926 Chemical Physics *6*, 4825-4831.
927 Dang, K.V., Plet, J., Tolleter, D., Jokel, M., Cuine, S., Carrier, P., Auroy, P., Richaud,
928 P., Johnson, X., Alric, J.*, et al.* (2014). Combined increases in mitochondrial
929 cooperation and oxygen photoreduction compensate for deficiency in cyclic electron
930 flow in Chlamydomonas reinhardtii. The Plant cell *26*, 3036-3050.
931 Danielsson, R., Suorsa, M., Paakkarinen, V., Albertsson, P.A., Styring, S., Aro, E.M.,
932 and Mamedov, F. (2006). Dimeric and monomeric organization of photosystem II.
933 Distribution of five distinct complexes in the different domains of the thylakoid
934 membrane. The Journal of biological chemistry *281*, 14241-14249.
935 Dent, R.M., Haglund, C.M., Chin, B.L., Kobayashi, M.C., and Niyogi, K.K. (2005).
936 Functional genomics of eukaryotic photosynthesis using insertional mutagenesis of
937 Chlamydomonas reinhardtii. Plant physiology *137*, 545-556.
938 Dinc, E., Ceppi, M.G., Toth, S.Z., Bottka, S., and Schansker, G. (2012). The chl a
939 fluorescence intensity is remarkably insensitive to changes in the chlorophyll content
940 of the leaf as long as the chl a/b ratio remains unaffected. Biochimica et biophysica
941 acta *1817*, 770-779.

942 Drop, B., Webber-Birungi, M., Fusetti, F., Kouril, R., Redding, K.E., Boekema, E.J.,
943 and Croce, R. (2011). Photosystem I of Chlamydomonas reinhardtii contains nine
944 light-harvesting complexes (Lhca) located on one side of the core. The Journal of
945 biological chemistry *286*, 44878-44887.
946 Drop, B., Webber-Birungi, M., Yadav, S.K., Filipowicz-Szymanska, A., Fusetti, F.,
947 Boekema, E.J., and Croce, R. (2014). Light-harvesting complex II (LHCII) and its
948 supramolecular organization in Chlamydomonas reinhardtii. Biochimica et biophysica
949 acta *1837*, 63-72.
950 Dumas, L., Chazaux, M., Peltier, G., Johnson, X., and Alric, J. (2016). Cytochrome b
951 6 f function and localization, phosphorylation state of thylakoid membrane proteins
952 and consequences on cyclic electron flow. Photosynthesis research *129*, 307-320.
953 Engel, B.D., Schaffer, M., Kuhn Cuellar, L., Villa, E., Plitzko, J.M., and Baumeister, W.
954 (2015). Native architecture of the Chlamydomonas chloroplast revealed by in situ
955 cryo-electron tomography. eLife *4*.
956 Erickson, E., Wakao, S., and Niyogi, K.K. (2015). Light stress and photoprotection in
957 Chlamydomonas reinhardtii. The Plant journal : for cell and molecular biology *82*,
958 449-465.
959 Farquhar, G.D., von Caemmerer, S., and Berry, J.A. (1980). A biochemical model of
960 photosynthetic CO2 assimilation in leaves of C 3 species. Planta *149*, 78-90.
961 Fischer, B.B., Dayer, R., Schwarzenbach, Y., Lemaire, S.D., Behra, R., Liedtke, A.,
962 and Eggen, R.I. (2009). Function and regulation of the glutathione peroxidase
963 homologous gene GPXH/GPX5 in Chlamydomonas reinhardtii. Plant molecular
964 biology *71*, 569-583.
965 Gonzalez-Ballester, D., de Montaigu, A., Galvan, A., and Fernandez, E. (2005).
966 Restriction enzyme site-directed amplification PCR: a tool to identify regions flanking
967 a marker DNA. Analytical biochemistry *340*, 330-335.
968 Goodenough, U.W., Armstrong, J.J., and Levine, R.P. (1969). Photosynthetic
969 Properties of ac-31, a Mutant Strain of Chlamydomonas reinhardi Devoid of
970 Chloroplast Membrane Stacking. Plant physiology *44*, 1001-1012.
971 Goodenough, U.W., and Levine, R.P. (1969). Chloroplast Ultrastructure in Mutant
972 Strains of Chlamydomonas reinhardi Lacking Components of the Photosynthetic
973 Apparatus. Plant physiology *44*, 990-1000.
974 Goodenough, U.W., and Staehelin, L.A. (1971). Structural differentiation of stacked
975 and unstacked chloroplast membranes. Freeze-etch electron microscopy of wild-type
976 and mutant strains of Chlamydomonas. The Journal of cell biology *48*, 594-619.
977 Guenther, J.E., and Melis, A. (1990). The physiological significance of photosystem II
978 heterogeneity in chloroplasts. Photosynthesis research *23*, 105-109.
979 Harris, E.H. (1989). The Chlamydomonas Sourcebook: A Comprehensive
980 Guide to Biology and Laboratory Use. (San Diego: Academic Press,).
981 Heinnickel, M.L., and Grossman, A.R. (2013). The GreenCut: re-evaluation of
982 physiological role of previously studied proteins and potential novel protein functions.
983 Photosynthesis research *116*, 427-436.
984 Herbstová, M., Tietz, S., Kinzel, C., Turkina, M.V., and Kirchhoff, H. (2012).
985 Architectural switch in plant photosynthetic membranes induced by light stress.
986 Proceedings of the National Academy of Sciences *109*, 20130-20135.
987 Huang, W., Chen, Q., Zhu, Y., Hu, F., Zhang, L., Ma, Z., He, Z., and Huang, J. (2013).
988 Arabidopsis thylakoid formation 1 is a critical regulator for dynamics of PSII-LHCII
989 complexes in leaf senescence and excess light. Molecular plant *6*, 1673-1691.

990 Jarvi, S., Suorsa, M., and Aro, E.M. (2015). Photosystem II repair in plant
991 chloroplasts--Regulation, assisting proteins and shared components with
992 photosystem II biogenesis. Biochimica et biophysica acta *1847*, 900-909.
993 Johnson, X., Steinbeck, J., Dent, R.M., Takahashi, H., Richaud, P., Ozawa, S.,
994 Houille-Vernes, L., Petroutsos, D., Rappaport, F., Grossman, A.R.*, et al.* (2014).
995 Proton gradient regulation 5-mediated cyclic electron flow under ATP- or redox-
996 limited conditions: a study of DeltaATpase pgr5 and DeltarbcL pgr5 mutants in the
997 green alga Chlamydomonas reinhardtii. Plant physiology *165*, 438-452.
998 Johnson, X., Vandystadt, G., Bujaldon, S., Wollman, F.A., Dubois, R., Roussel, P.,
999 Alric, J., and Beal, D. (2009). A new setup for in vivo fluorescence imaging of
1000 photosynthetic activity. Photosynthesis research *102*, 85-93.
1001 Johnson, X., Wostrikoff, K., Finazzi, G., Kuras, R., Schwarz, C., Bujaldon, S.,
1002 Nickelsen, J., Stern, D.B., Wollman, F.A., and Vallon, O. (2010). MRL1, a conserved
1003 Pentatricopeptide repeat protein, is required for stabilization of rbcL mRNA in
1004 Chlamydomonas and Arabidopsis. The Plant cell *22*, 234-248.
1005 Kallberg, M., Wang, H., Wang, S., Peng, J., Wang, Z., Lu, H., and Xu, J. (2012).
1006 Template-based protein structure modeling using the RaptorX web server. Nature
1007 protocols *7*, 1511-1522.
1008 Khan, N.Z., Lindquist, E., and Aronsson, H. (2013). New putative chloroplast vesicle
1009 transport components and cargo proteins revealed using a bioinformatics approach:
1010 an Arabidopsis model. PloS one *8*, e59898.
1011 Khatoon, M., Inagawa, K., Pospisil, P., Yamashita, A., Yoshioka, M., Lundin, B., Horie,
1012 J., Morita, N., Jajoo, A., Yamamoto, Y.*, et al.* (2009). Quality control of photosystem II:
1013 Thylakoid unstacking is necessary to avoid further damage to the D1 protein and to
1014 facilitate D1 degradation under light stress in spinach thylakoids. The Journal of
1015 biological chemistry *284*, 25343-25352.
1016 Kirchhoff, H. (2019). Chloroplast ultrastructure in plants. The New phytologist *223*,
1017 565-574.
1018 Komenda, J., and Sobotka, R. (2016). Cyanobacterial high-light-inducible proteins--
1019 Protectors of chlorophyll-protein synthesis and assembly. Biochimica et biophysica
1020 acta *1857*, 288-295.
1021 Koochak, H., Puthiyaveetil, S., Mullendore, D.L., Li, M., and Kirchhoff, H. (2019). The
1022 structural and functional domains of plant thylakoid membranes. The Plant journal :
1023 for cell and molecular biology *97*, 412-429.
1024 Kouril, R., Lukas, N., Semchonok, D.A., Boekema, E.J., and Ilik, P. (2018).
1025 Membrane Protein Complexes: Structure and Function. In Subcellular Biochemistry,
1026 E.J.B. J. Robin Harris, ed. (Singapore: Springer), p. 459.
1027 Kouril, R., Wientjes, E., Bultema, J.B., Croce, R., and Boekema, E.J. (2013). High-
1028 light vs. low-light: effect of light acclimation on photosystem II composition and
1029 organization in Arabidopsis thaliana. Biochimica et biophysica acta *1827*, 411-419.
1030 Larosa, V., Meneghesso, A., La Rocca, N., Steinbeck, J., Hippler, M., Szabo, I., and
1031 Morosinotto, T. (2018). Mitochondria Affect Photosynthetic Electron Transport and
1032 Photosensitivity in a Green Alga. Plant physiology *176*, 2305-2314.
1033 Li, X., Zhang, R., Patena, W., Gang, S.S., Blum, S.R., Ivanova, N., Yue, R.,
1034 Robertson, J.M., Lefebvre, P.A., Fitz-Gibbon, S.T.*, et al.* (2016). An Indexed, Mapped
1035 Mutant Library Enables Reverse Genetics Studies of Biological Processes in
1036 Chlamydomonas reinhardtii. The Plant cell *28*, 367-387.
1037 Lu, Y. (2016). Identification and Roles of Photosystem II Assembly, Stability, and
1038 Repair Factors in Arabidopsis. Frontiers in plant science *7*, 168.

Majeran, W., Zybailov, B., Ytterberg, A.J., Dunsmore, J., Sun, Q., and van Wijk, K.J. (2008). Consequences of C4 differentiation for chloroplast membrane proteomes in maize mesophyll and bundle sheath cells. Molecular & cellular proteomics : MCP *7*, 1609-1638.

Melis, A. (1991). Dynamics of photosynthetic membrane composition and function. Biochimica et biophysica acta *1058*, 87–106.

Melis, A. (1996). Excitation energy transfer: functional and dynamic aspects of Lhc (cab) proteins. In Oxygenic Photosynthesis: The Light Reactions Volume 4 of Advances in Photosynthesis and Respiration, D.R. Ort, and C.F. Yocum, eds. (Dordrecht, The Netherlands: Kluwer Academic Publishers), pp. 523–538.

Melis, A., and Homann, P.H. (1976). Heterogeneity of the Photochemical centres in system II of Chloroplasts Photochemistry and Photobiology *23*, 343-350.

Merchant, S.S., Prochnik, S.E., Vallon, O., Harris, E.H., Karpowicz, S.J., Witman, G.B., Terry, A., Salamov, A., Fritz-Laylin, L.K., Marechal-Drouard, L.*, et al.* (2007). The Chlamydomonas genome reveals the evolution of key animal and plant functions. Science *318*, 245-250.

Michaeli, S., Honig, A., Levanony, H., Peled-Zehavi, H., and Galili, G. (2014). Arabidopsis ATG8-INTERACTING PROTEIN1 is involved in autophagy-dependent vesicular trafficking of plastid proteins to the vacuole. The Plant cell *26*, 4084-4101.

Mulkidjanian, A.Y., Koonin, E.V., Makarova, K.S., Mekhedov, S.L., Sorokin, A., Wolf, Y.I., Dufresne, A., Partensky, F., Burd, H., Kaznadzey, D.*, et al.* (2006). The cyanobacterial genome core and the origin of photosynthesis. Proceedings of the National Academy of Sciences of the United States of America *103*, 13126-13131.

Munekage, Y.N., Genty, B., and Peltier, G. (2008). Effect of PGR5 impairment on photosynthesis and growth in Arabidopsis thaliana. Plant & cell physiology *49*, 1688-1698.

Muranaka, L.S., Rutgers, M., Bujaldon, S., Heublein, A., Geimer, S., Wollman, F.A., and Schroda, M. (2016). TEF30 Interacts with Photosystem II Monomers and Is Involved in the Repair of Photodamaged Photosystem II in Chlamydomonas reinhardtii. Plant physiology *170*, 821-840.

Myouga, F., Takahashi, K., Tanaka, R., Nagata, N., Kiss, A.Z., Funk, C., Nomura, Y., Nakagami, H., Jansson, S., and Shinozaki, K. (2018). Stable Accumulation of Photosystem II Requires ONE-HELIX PROTEIN1 (OHP1) of the Light Harvesting-Like Family. Plant physiology *176*, 2277-2291.

Nawrocki, W.J., Liu, X., and Croce, R. (2020). Chlamydomonas reinhardtii Exhibits De Facto Constitutive NPQ Capacity in Physiologically Relevant Conditions. Plant physiology *182*, 472-479.

Pagliano, C., Barera, S., Chimirri, F., Saracco, G., and Barber, J. (2012). Comparison of the alpha and beta isomeric forms of the detergent n-dodecyl-D-maltoside for solubilizing photosynthetic complexes from pea thylakoid membranes. Biochimica et biophysica acta *1817*, 1506-1515.

Plochinger, M., Schwenkert, S., von Sydow, L., Schroder, W.P., and Meurer, J. (2016). Functional Update of the Auxiliary Proteins PsbW, PsbY, HCF136, PsbN, TerC and ALB3 in Maintenance and Assembly of PSII. Frontiers in plant science *7*, 423.

Polukhina, I., Fristedt, R., Dinc, E., Cardol, P., and Croce, R. (2016). Carbon Supply and Photoacclimation Cross Talk in the Green Alga Chlamydomonas reinhardtii. Plant physiology *172*, 1494-1505.

Pribil, M., Labs, M., and Leister, D. (2014). Structure and dynamics of thylakoids in land plants. J Exp Bot *65*, 1955-1972.

1089 Pribil, M., Sandoval-Ibanez, O., Xu, W., Sharma, A., Labs, M., Liu, Q., Galgenmuller,
1090 C., Schneider, T., Wessels, M., Matsubara, S., *et al.* (2018). Fine-Tuning of
1091 Photosynthesis Requires CURVATURE THYLAKOID1-Mediated Thylakoid Plasticity.
1092 Plant physiology *176*, 2351-2364.
1093 Rexroth, S., Meyer zu Tittingdorf, J.M., Krause, F., Dencher, N.A., and Seelert, H.
1094 (2003). Thylakoid membrane at altered metabolic state: challenging the forgotten
1095 realms of the proteome. Electrophoresis *24*, 2814-2823.
1096 Rexroth, S., Mullineaux, C.W., Ellinger, D., Sendtko, E., Rogner, M., and Koenig, F.
1097 (2011). The plasma membrane of the cyanobacterium Gloeobacter violaceus
1098 contains segregated bioenergetic domains. The Plant cell *23*, 2379-2390.
1099 Roach, T., Baur, T., Stoggl, W., and Krieger-Liszkay, A. (2017). Chlamydomonas
1100 reinhardtii responding to high light: a role for 2-propenal (acrolein). Physiologia
1101 plantarum *161*, 75-87.
1102 Rochaix, J.D. (2014). Regulation and dynamics of the light-harvesting system. Annual
1103 review of plant biology *65*, 287-309.
1104 Rozak, P.R., Seiser, R.M., Wacholtz, W.F., and Wise, R.R. (2002). Rapid, reversible
1105 alterations in spinach thylakoid appression upon changes in light intensity. Plant, Cell
1106 and Environment *25*, 421-429.
1107 Schroda, M., Beck, C.F., and Vallon, O. (2002). Sequence elements within an HSP70
1108 promoter counteract transcriptional transgene silencing in Chlamydomonas. The
1109 Plant journal : for cell and molecular biology *31*, 445-455.
1110 Schwarz, E.M., Tietz, S., and Froehlich, J.E. (2018). Photosystem I-LHCII
1111 megacomplexes respond to high light and aging in plants. Photosynthesis research
1112 *136*, 107-124.
1113 Semchonok, D.A., Sathish Yadav, K.N., Xu, P., Drop, B., Croce, R., and Boekema,
1114 E.J. (2017). Interaction between the photoprotective protein LHCSR3 and C2S2
1115 Photosystem II supercomplex in Chlamydomonas reinhardtii. Biochimica et
1116 biophysica acta Bioenergetics *1858*, 379-385.
1117 Shen, L., Huang, Z., Chang, S., Wang, W., Wang, J., Kuang, T., Han, G., Shen, J.R.,
1118 and Zhang, X. (2019). Structure of a C2S2M2N2-type PSII-LHCII supercomplex from
1119 the green alga Chlamydomonas reinhardtii. Proceedings of the National Academy of
1120 Sciences of the United States of America *116*, 21246-21255.
1121 Shi, L.X., Hall, M., Funk, C., and Schroder, W.P. (2012). Photosystem II, a growing
1122 complex: updates on newly discovered components and low molecular mass
1123 proteins. Biochimica et biophysica acta *1817*, 13-25.
1124 Sizova, I., Fuhrmann, M., and Hegemann, P. (2001). A Streptomyces rimosus aphVIII
1125 gene coding for a new type phosphotransferase provides stable antibiotic resistance
1126 to Chlamydomonas reinhardtii. Gene *277*, 221-229.
1127 Stark, H. (2010). GraFix: stabilization of fragile macromolecular complexes for single
1128 particle cryo-EM. Methods in enzymology *481*, 109-126.
1129 Su, X., Ma, J., Wei, X., Cao, P., Zhu, D., Chang, W., Liu, Z., Zhang, X., and Li, M.
1130 (2017). Structure and assembly mechanism of plant C2S2M2-type PSII-LHCII
1131 supercomplex. Science *357*, 815-820.
1132 Suorsa, M., Rantala, M., Mamedov, F., Lespinasse, M., Trotta, A., Grieco, M., Vuorio,
1133 E., Tikkanen, M., Jarvi, S., and Aro, E.M. (2015). Light acclimation involves dynamic
1134 re-organization of the pigment-protein megacomplexes in non-appressed thylakoid
1135 domains. The Plant journal : for cell and molecular biology *84*, 360-373.
1136 Terashima, M., Specht, M., and Hippler, M. (2011). The chloroplast proteome: a
1137 survey from the Chlamydomonas reinhardtii perspective with a focus on distinctive
1138 features. Current genetics *57*, 151-168.

Theis, J., and Schroda, M. (2016). Revisiting the photosystem II repair cycle. Plant Signaling & Behavior *11*, e1218587.

Thornton, L.E., Ohkawa, H., Roose, J.L., Kashino, Y., Keren, N., and Pakrasi, H.B. (2004). Homologs of plant PsbP and PsbQ proteins are necessary for regulation of photosystem ii activity in the cyanobacterium Synechocystis 6803. The Plant cell *16*, 2164-2175.

Tibiletti, T., Auroy, P., Peltier, G., and Caffarri, S. (2016). Chlamydomonas reinhardtii PsbS Protein Is Functional and Accumulates Rapidly and Transiently under High Light. Plant physiology *171*, 2717-2730.

Tomizioli, M., Lazar, C., Brugiere, S., Burger, T., Salvi, D., Gatto, L., Moyet, L., Breckels, L.M., Hesse, A.M., Lilley, K.S.*, et al.* (2014). Deciphering thylakoid sub-compartments using a mass spectrometry-based approach. Molecular & cellular proteomics : MCP *13*, 2147-2167.

Torabi, S., Umate, P., Manavski, N., Plochinger, M., Kleinknecht, L., Bogireddi, H., Herrmann, R.G., Wanner, G., Schroder, W.P., and Meurer, J. (2014). PsbN is required for assembly of the photosystem II reaction center in Nicotiana tabacum. The Plant cell *26*, 1183-1199.

Tyystjarvi, E., and Aro, E.M. (1996). The rate constant of photoinhibition, measured in lincomycin-treated leaves, is directly proportional to light intensity. Proceedings of the National Academy of Sciences of the United States of America *93*, 2213-2218.

Umena, Y., Kawakami, K., Shen, J.R., and Kamiya, N. (2011). Crystal structure of oxygen-evolving photosystem II at a resolution of 1.9 A. Nature *473*, 55-60.

Walters, R.G. (2005). Towards an understanding of photosynthetic acclimation. J Exp Bot *56*, 435-447.

Walters, R.G., Shephard, F., Rogers, J.J., Rolfe, S.A., and Horton, P. (2003). Identification of mutants of Arabidopsis defective in acclimation of photosynthesis to the light environment. Plant physiology *131*, 472-481.

Wang, L., Yamano, T., Takane, S., Niikawa, Y., Toyokawa, C., Ozawa, S.I., Tokutsu, R., Takahashi, Y., Minagawa, J., Kanesaki, Y.*, et al.* (2016). Chloroplast-mediated regulation of CO2-concentrating mechanism by Ca2+-binding protein CAS in the green alga Chlamydomonas reinhardtii. Proceedings of the National Academy of Sciences of the United States of America *113*, 12586-12591.

Wei, X., Su, X., Cao, P., Liu, X., Chang, W., Li, M., Zhang, X., and Liu, Z. (2016). Structure of spinach photosystem II-LHCII supercomplex at 3.2 A resolution. Nature *534*, 69-74.

Yang, D.H., Webster, J., Adam, Z., Lindahl, M., and Andersson, B. (1998). Induction of acclimative proteolysis of the light-harvesting chlorophyll a/b protein of photosystem II in response to elevated light intensities. Plant physiology *118*, 827-834.

Zehr, J.P., Bench, S.R., Carter, B.J., Hewson, I., Niazi, F., Shi, T., Tripp, H.J., and Affourtit, J.P. (2008). Globally distributed uncultivated oceanic N2-fixing cyanobacteria lack oxygenic photosystem II. Science *322*, 1110-1112.

Zhang, R., Patena, W., Armbruster, U., Gang, S.S., Blum, S.R., and Jonikas, M.C. (2014). High-Throughput Genotyping of Green Algal Mutants Reveals Random Distribution of Mutagenic Insertion Sites and Endonucleolytic Cleavage of Transforming DNA. The Plant cell *26*, 1398-1409.

Figure 1.

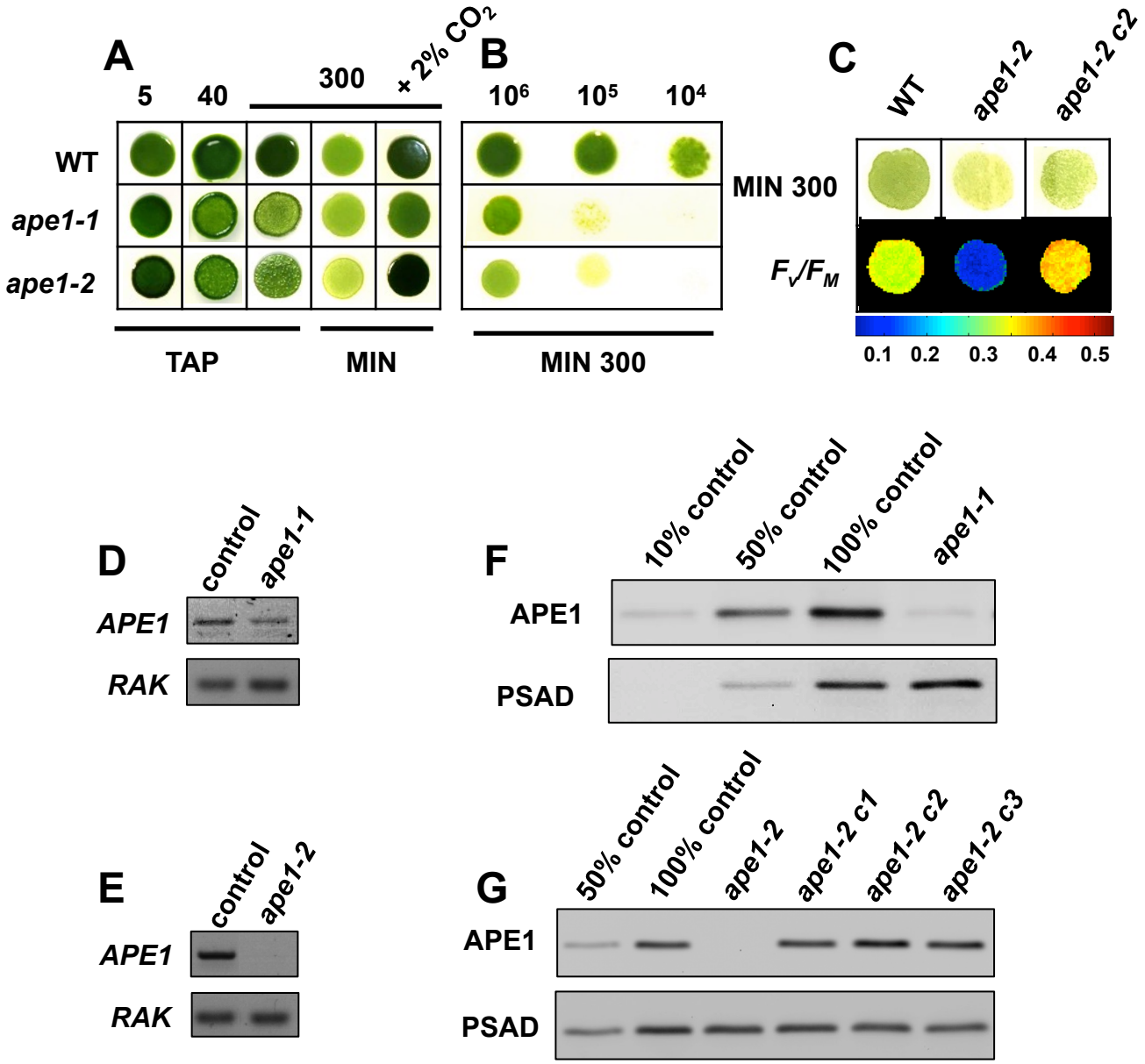

Figure 1. Identification of *ape1* alleles that are interrupted in *Cre16.g665250* encoding APE1, a protein that contributes to optimal growth in high light. A. Spot tests (10^6 cells.mL^{-1}) on rich media (TAP) versus minimal media (MIN) at different light intensities and with or without supplement of 2% CO_2. **B.** Dilution series of cells grown at high light (300 $\mu mol_{photons}.m^{-2}.s^{-1}$) on minimal media. **C.** Growth and maximum PSII quantum yield on minimal media grown at high light. The false color images give a range for the F_V/F_M value. **D.** RT-PCR on control lines, *ape1-1* and **E.** *ape1-2* using *RAK* gene as a positive control and primers E and F (see Supplemental Figure 1) for *APE1*. **F.** APE1 immunoblot of total cell proteins of control line and wild type versus *ape1-1* and **G.** *ape1-2* and three complemented lines. PSAD was used as a loading control.

Figure 2.

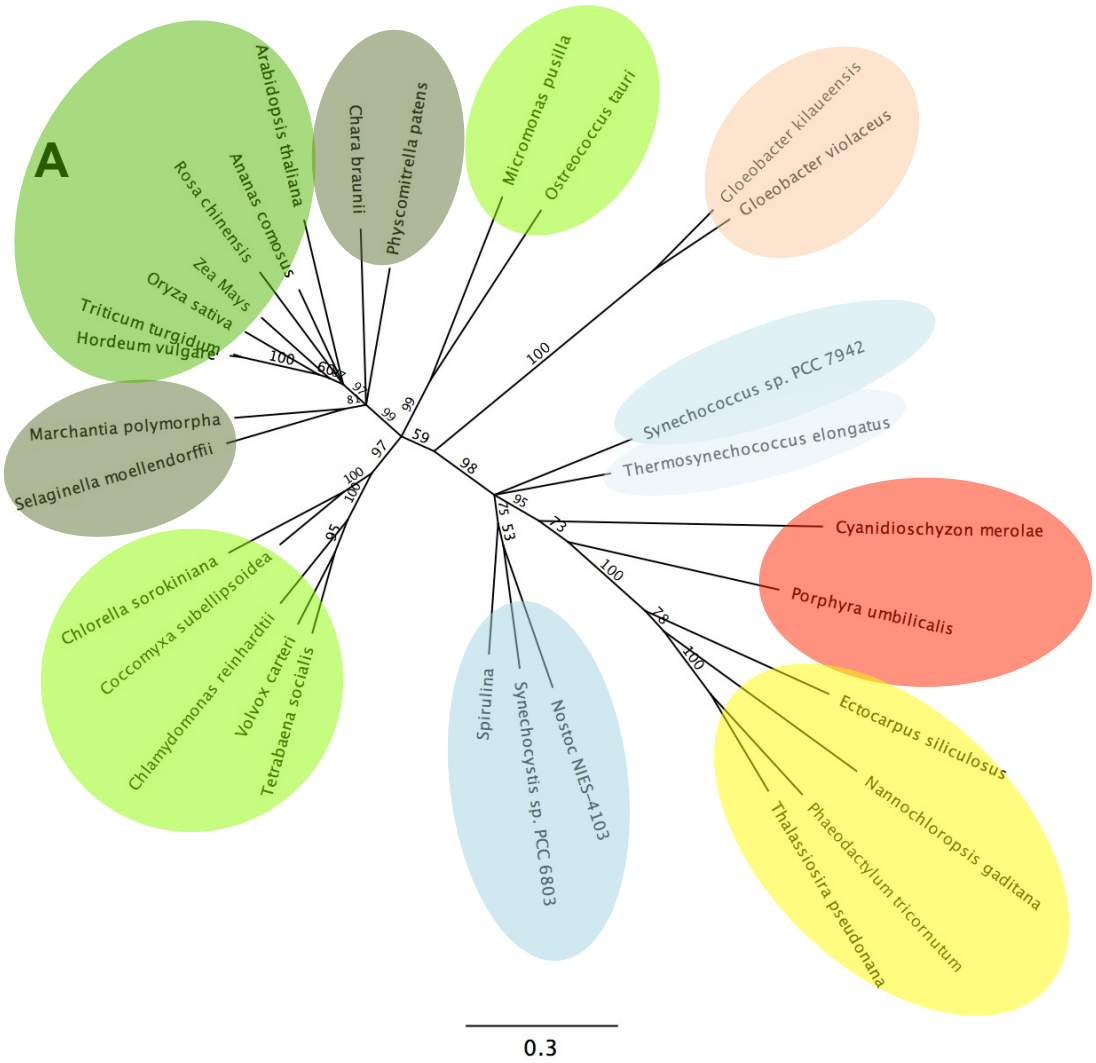

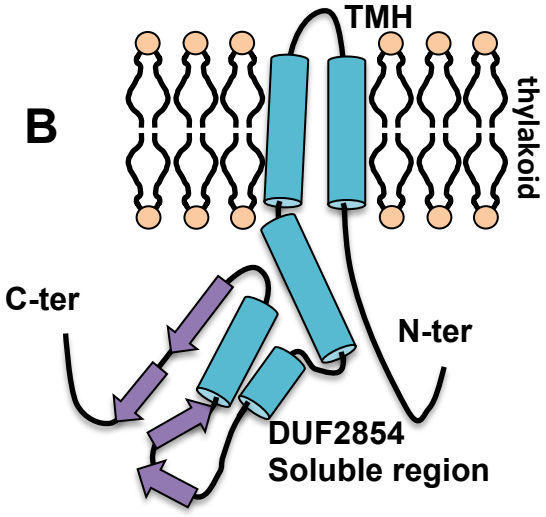

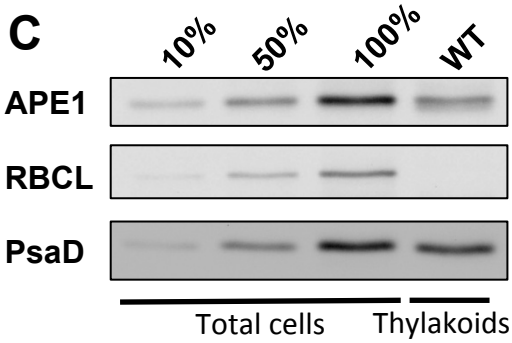

Figure 2. APE1 is a thylakoid protein present in all oxygenic phototrophs. A. Cladogram of APE1: Representative APE1 protein sequences from all clades of oxygenic photosynthetic species were identified by BLAST, alignment was done using Geneious (MUSCLE Alignment). The cladogram was constructed using a Jukes-Cantor genetic distance model neighbor-joining tree build method, unrooted, with Bootstrap consensus shown on branches. Colour codes represent phylum and distribution: green: land plants; army green: primitive plants; pale green: green algae; pale pink: primitive cyanobacteria; pale blue: hot spring cyanobacteria; blue: marine cyanobacteria; darker blue; fresh water cynaobacteria; pink: red algae; yellow: heterokont algae. **B.** Secondary structure model of the APE1 protein in the thylakoid lipid bilayer showing predicted (RaptorX) transmembrane and alpha helices (in blue) and beta-coil (in purple). **C.** Immunoblot of APE1 in total cells and thylakoids of the wild type. RBCL was used as a stromal control; PSAD was used as a thylakoid control.

Figure 3.

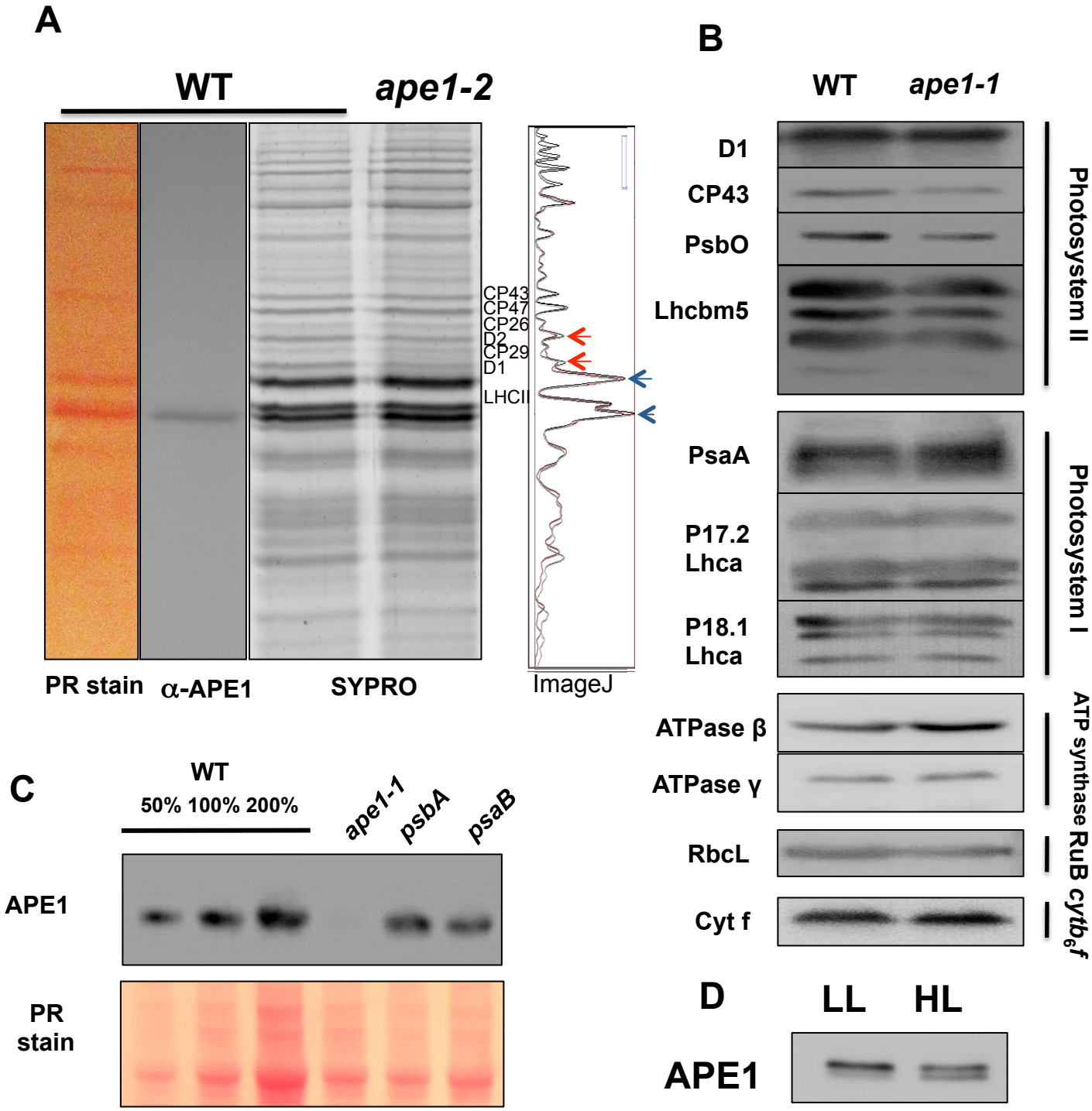

Figure 3. APE1 contributes to PSII accumulation but is not required for photosystem biogenesis. A. Thylakoid proteins were isolated from WT and *ape1-2* grown under low light (10 $\mu mol_{photons}.m^{-2}.s^{-1}$) in heterotrophic conditions and separated using denaturing gels (15.5% 6M Urea) that were used for immunoblot of APE1 and for SYPRO staining. PSII proteins, minor antennae and LHCII were identified and quantified using image analysis (ImageJ). **B.** Immunoblot analysis of major photosynthetic complexes shown for wildtype and *ape1-1* grown at low light (80 $\mu mol_{photons}.m^{-2}.s^{-1}$ under phototrophic conditions). **C.** Immunoblot analysis of APE1 accumulation in *ape1-1*, and mutants lacking PSII (*psbA*) and PSI (*psaB*). Ponceau Red was used as a loading control**. D.** Cells were sampled from photobioreactors at low (LL) and high light (HL) at the same cellular density and loaded onto denaturing gels. Western blot analysis was used to measure APE1 accumulation and bands were quantified using ImageJ.

Figure 4.

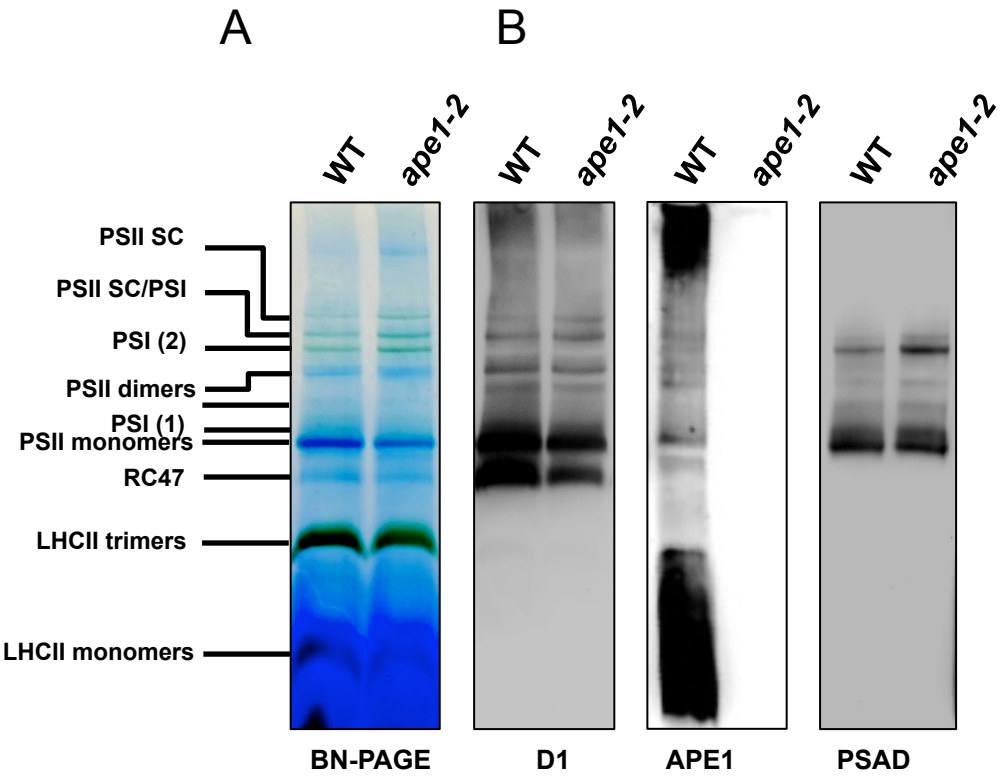

Figure 4. APE1 affects the distribution of high molecular mass photosystem complexes and the APE1 protein co-migrates with PSII. A. Analysis of native protein complex formation of WT and *ape1-2* cells grown phototrophically in low light. Thylakoid membrane proteins were solubilized using 0.5% digitonin/0.5% α-DM and separated by BN-PAGE (4-16%). Proteins were loaded on a per chlorophyll basis. **B.** Immunoblot analysis of the BN-PAGE in (A.) using antisera against D1 protein, APE1 and PSAD**.**

Figure 5.

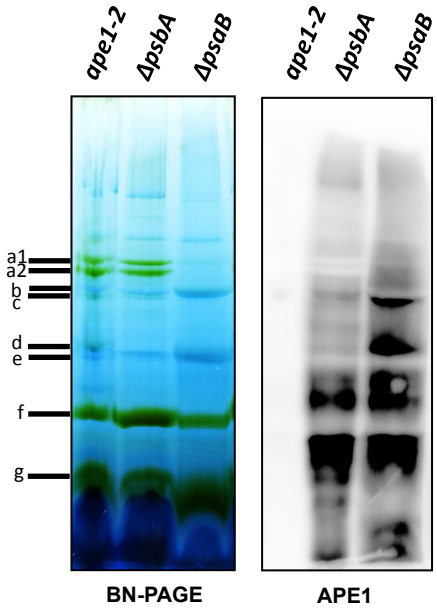

Figure 5. BN-PAGE (3-12%) analysis of *psbA* and *psaB* mutants grown heterotrophically in low light (10 $\mu mol_{photons}.m^{-2}.s^{-1}$) with thylakoids isolated and treated under the same conditions as in Figure 4 and immunblot analysis using the APE1 antibody. Labelled bands were identified by excising the lanes and separation by SDS-PAGE in the second dimension : a1, PSI; a2, PSI; b, PSII dimers; c, PSI core; d, PSII monomers; e, cytb_6f; f, LHCII trimers; g, LHCII monomers.

Figure 6.

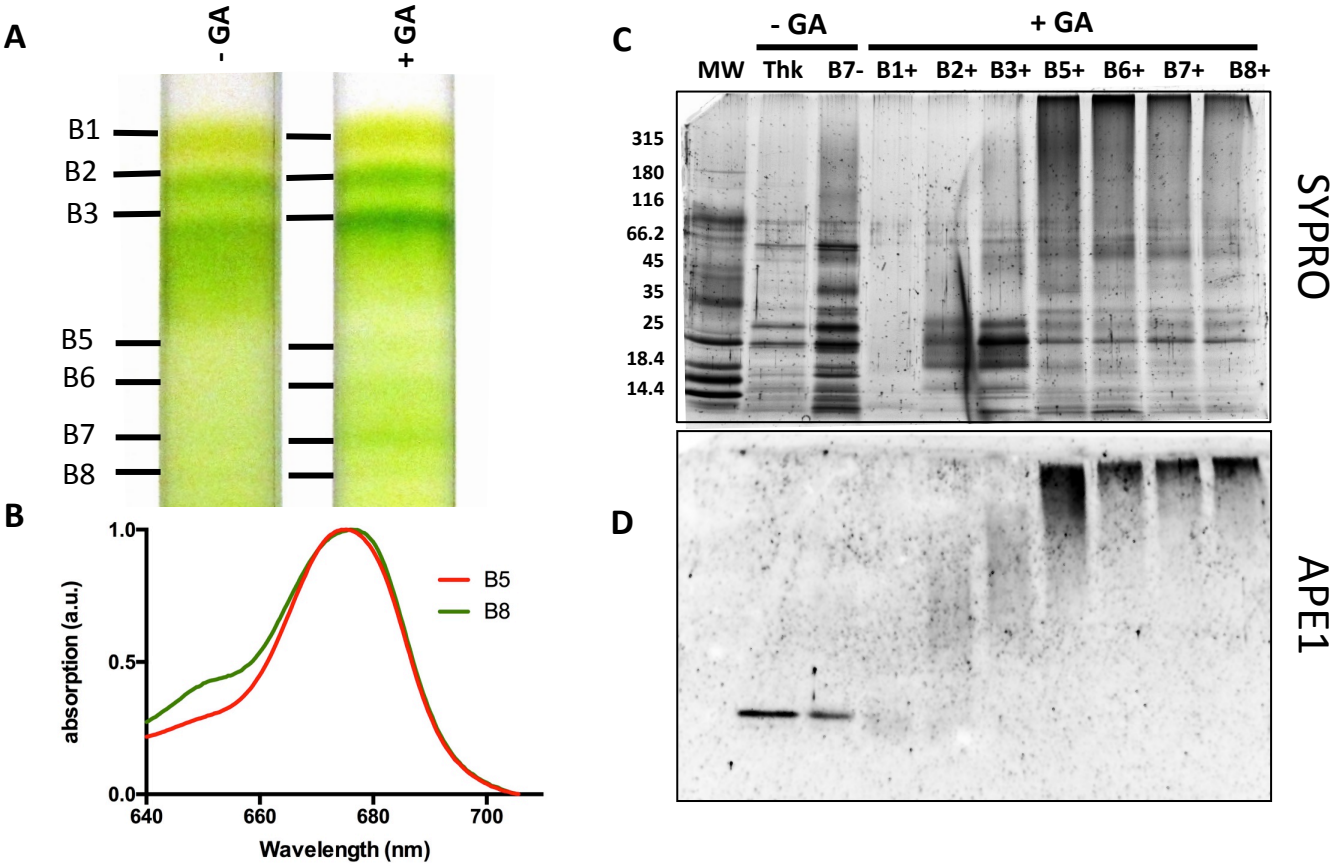

Figure 6. Crosslinking of native thylakoid complexes reveals the interaction between APE1 and PSII core. A. Thylakoid membranes extracted from wildtype cells grown phototrophically in low light were solubilized in 1% α-DM and 1% Digitonin, and loaded on sucrose gradients, with or without addition of glutaraldehyde (GA) as a crosslinker and subjected to ultracentrifugation. Labeled bands were isolated by syringe and these fractions were identified by their absorption spectra. **B.** absorption spectra at room temperature of the fractions B5 and fraction B8 from sucrose gradients. The spectra were normalised to maxima and minima in the 640-710 nm region. **C.** The different fractions with or without addition of glutaraldehyde (GA) shown in (A.) were analyzed by denaturing SDS-PAGE and stained with SYPRO, alongside the molecular weight marker (MW) and a sample of the non-treated thylakoid membranes (Thk). **D.** Immunoblot analysis of the gel shown in (B.) decorated with the APE1 antibody.

Figure 7.

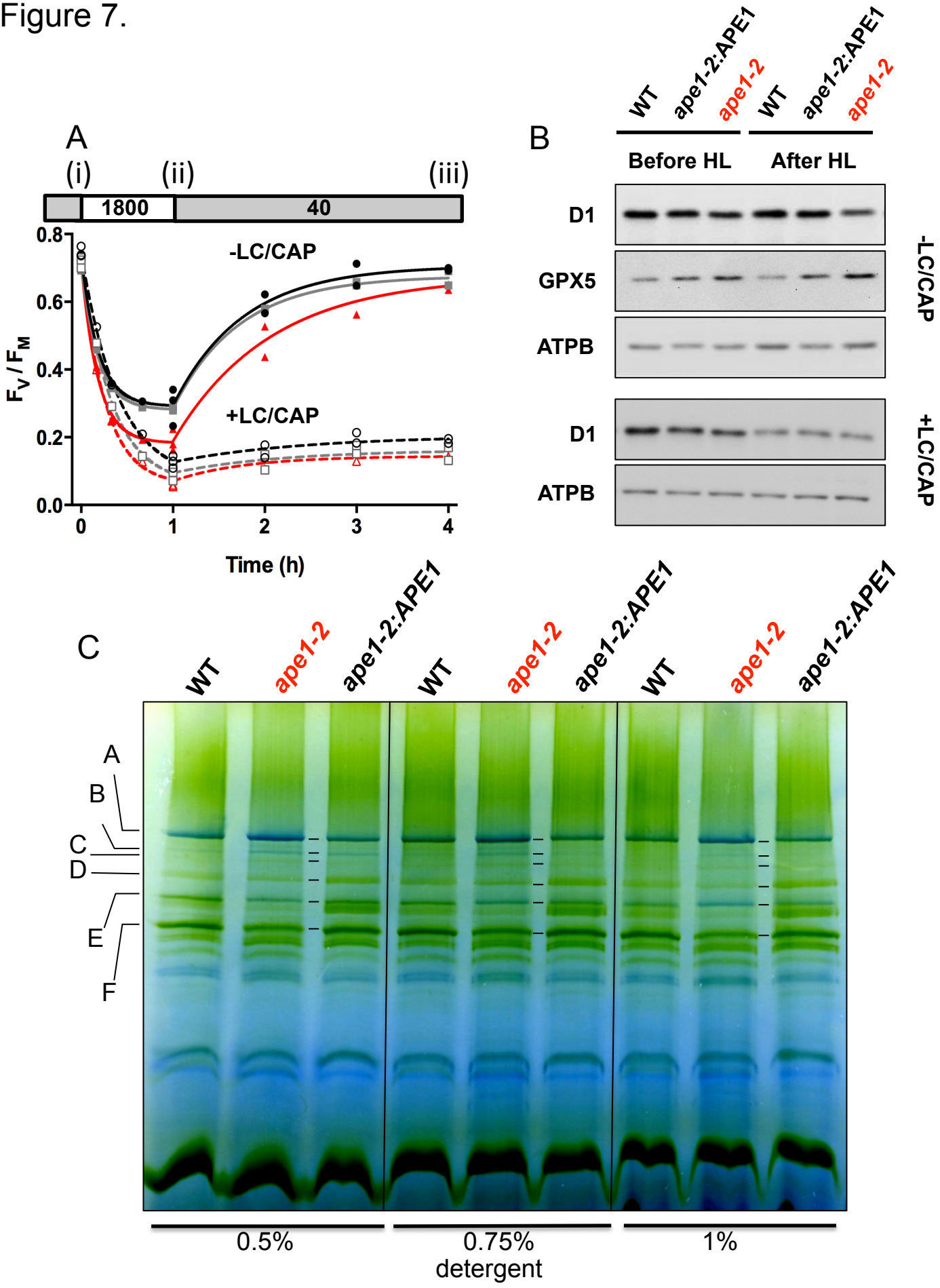

Figure 7. APE1 protects against photoinhibition. A. The wild type (black solid line), *ape1-2* complemented (grey solid line) and *ape1-2* (red solid line) strains in TAP media at the same cellular density were placed at (i) 40 $\mu mol_{photons}.m^{-2}.s^{-1}$ for 60 min, (ii) photoinhibited (PI) for 60 min at 1,800 $\mu mol_{photons}.m^{-2}.s^{-1}$, and then (iii) allowed to recover at 40 $\mu mol_{photons}.m^{-2}.s^{-1}$. PSII fluorescence was measured by pulse amplitude-modulated fluorometry. Lincomycin and chloramphenicol were added (+LC/CAP) to inhibit translation of chloroplastic proteins (dashed lines). Two replicates are shown and curves were fitted using a single exponential. **B.** Immunoblot analysis of D1 and GPX5 (monitoring ROS production) accumulation during the experiment shown in (A.), before and after the high light treatment, both without and with inhibitors of protein translation. ATPB was used as a loading control. **C.** Cells from *ape1-2*, WT and *ape1-2*:APE1 were grown phototrophically in batch cultures at ambient CO_2 at low light and then subjected to high light (300 $\mu mol_{photons}.m^{-2}.s^{-1}$) overnight (16 hours). Thylakoids were isolated and the concentration of the solubilizing agents α-DM and digitonin were varied from 0.5 to 1 % for the same concentration of chlorophyll per sample and separated by BN PAGE (3-12%). The complexes showing the major differences between the *ape1-2* and the control lines were identified in *ape1-2* and represented by the letters: . A. PSII SC, PSI, mitoATPsynthase, B. PSII SC, mitoATPsynthase, C. PSII SC, mitoATPsynthase, D. PSII SC, mitoATPsynthase, E. PSII core dimers, LHCII, PSI, F. PSI

Figure 8.

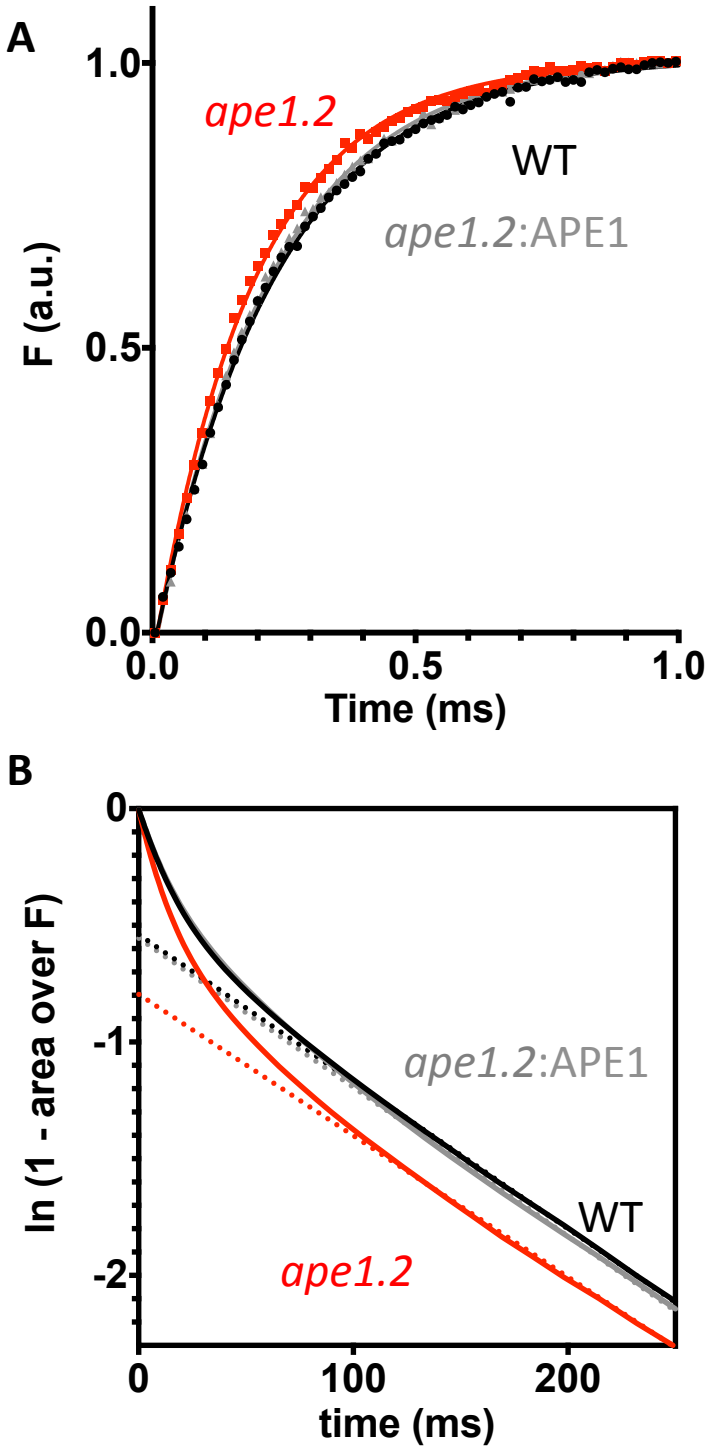

Figure 8. Differences in effective antenna size can be measured *in vivo* between wild type (black), *ape1-2* (red) and *ape1-2*: APE1 (grey) **A.** A typical fluorescence rise (F) for intact cells at room temperature pre-treated with high light (500 µmol photons.m^{-2}.s^{-1}) with recovery in low light (40 µmol photons.m^{-2}.s^{-1}) as in (iii) Figure 7. Actinic light was 8000 µmol photons.m^{-2}.s^{-1}. Data is normalized with F = 0-1 **B.** Estimation of the relative fraction of α-centers, i.e. large antenna size Photosystem II. The bi-phasic Q_A reduction rate as the time-dependent complementary area over the fluorescence rise, shown in logarithmic scale. Dotted lines intercept the ordinate axis at t = 0, yielding 55% α-centres for *ape1-2* and 42% for wild type and *ape1-2*:APE1. The experiements shown are representative of n>3 showing similar trends.

Figure 9.

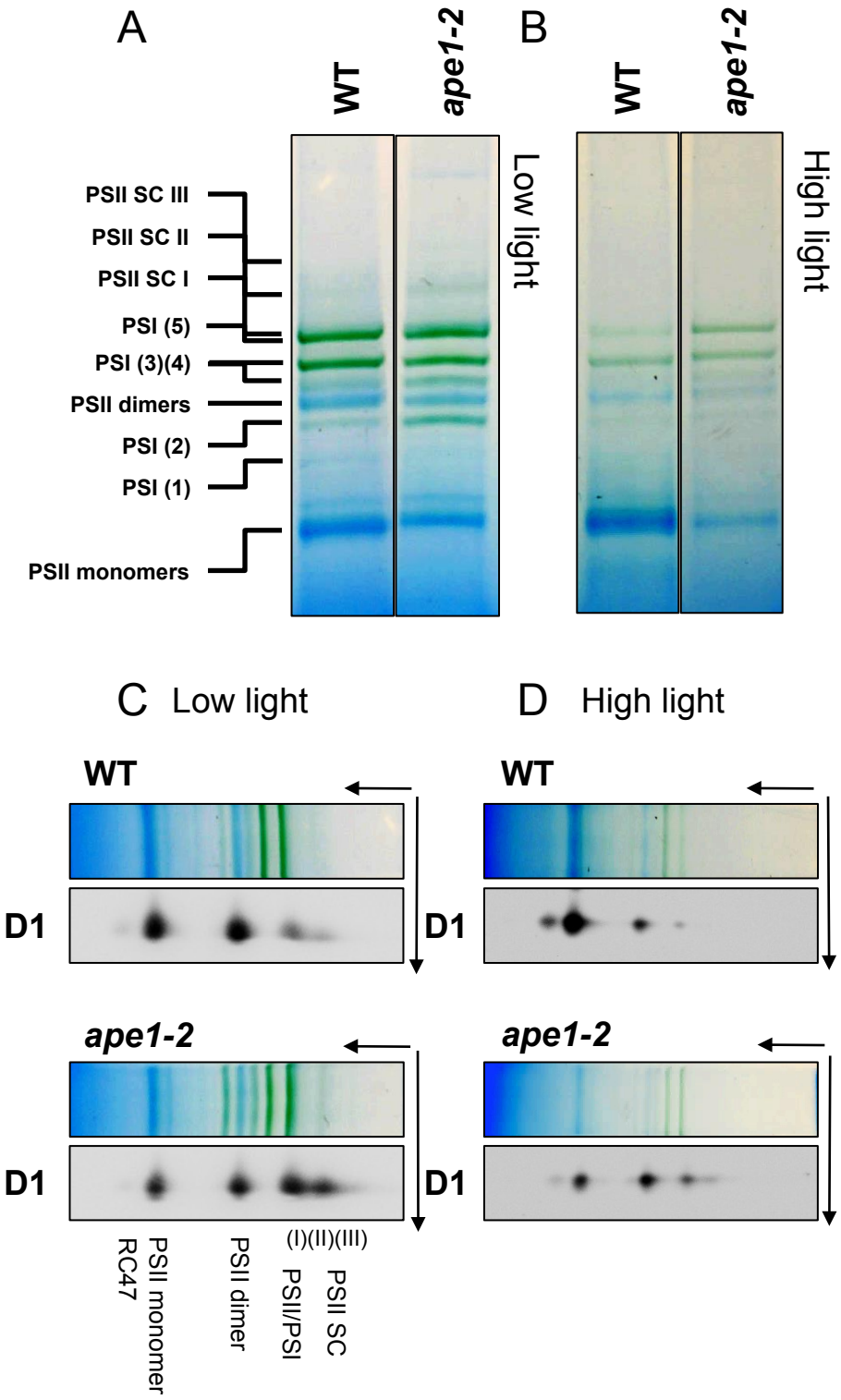

Figure 9. APE1 participates in the mobility of PSII complexes towards core monomers in response to an acclimation to high light A. BN-PAGE analysis of thylakoid proteins from wild type and *ape1-2* cells acclimated to low light and **B.** acclimated to high light. Thylakoid membrane proteins were solubilized using 1% β-DM and Digitonin and separated by BN-PAGE (4-16%). Proteins were loaded on a per chlorophyll basis. **C.** and **D.** The second dimension analysis was performed by excising and dentauring the BN-PAGE lane and proteins were separated by SDS-PAGE followed by immunoblotting using antisera against PSII D1 protein.

Figure 10.

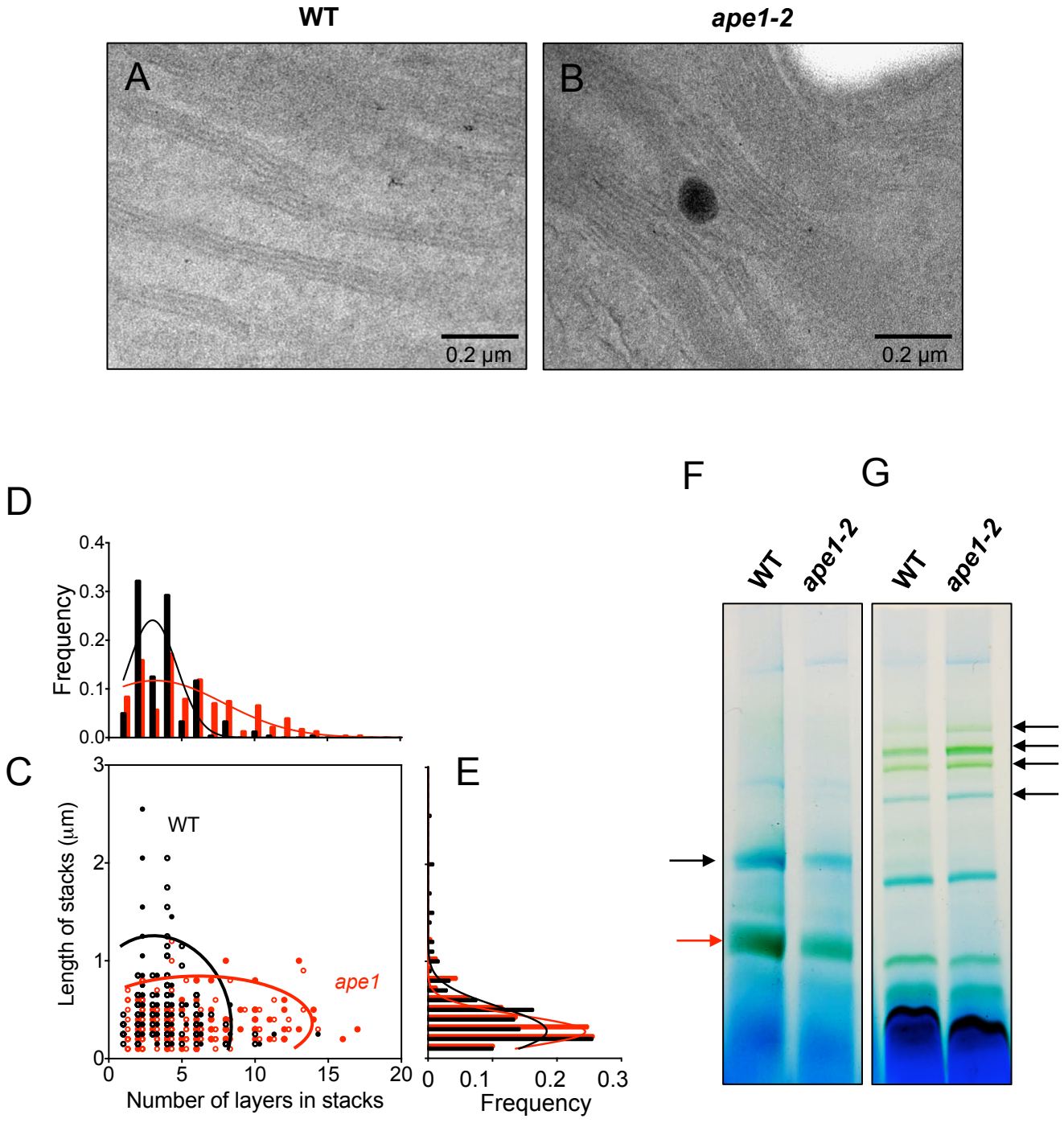

Figure 10. *ape1* has shorter thylakoid stacks composed of more layers, its thylakoids are enriched in grana cores in comparison to end membranes and stromal lamellae. Transmission Electron Microscope images of thylakoids of **A.** wild type and **B.** *ape1-2* from cells acclimated phototrophically in turbidostats at low light and ambient CO_2. **C.** Comparison of the stacking of thylakoid membranes between *ape1-2* and wild type. The length of a stack is represented against the number of layers as a scatter plot with 95% confidence ellipses calculated with Mathlab. **D.** and **E.** Data are projected into a single dimension giving the distribution of the number of layers and the length of the stacks with bell curves. Analysis is representative of 450 stacks and 85 TEM images. **F.** Differential solubilization of thylakoids of cells grown phototrophically at low light in batch cultures. Thylakoid membrane proteins were first solubilized using 1% digitonin to isolate end membranes and stromal lamellae and separated by BN-PAGE. Red arrow LHCII, balck arrow PSII **G.** The remaining pellet containing mostly stacked regions was then solubilized with 1% β-DM and separated by BN-PAGE. Arrows show differential accumulation of PSII enriched bands between the mutant and wild type in the two solubilized fractions.

Figure 11.

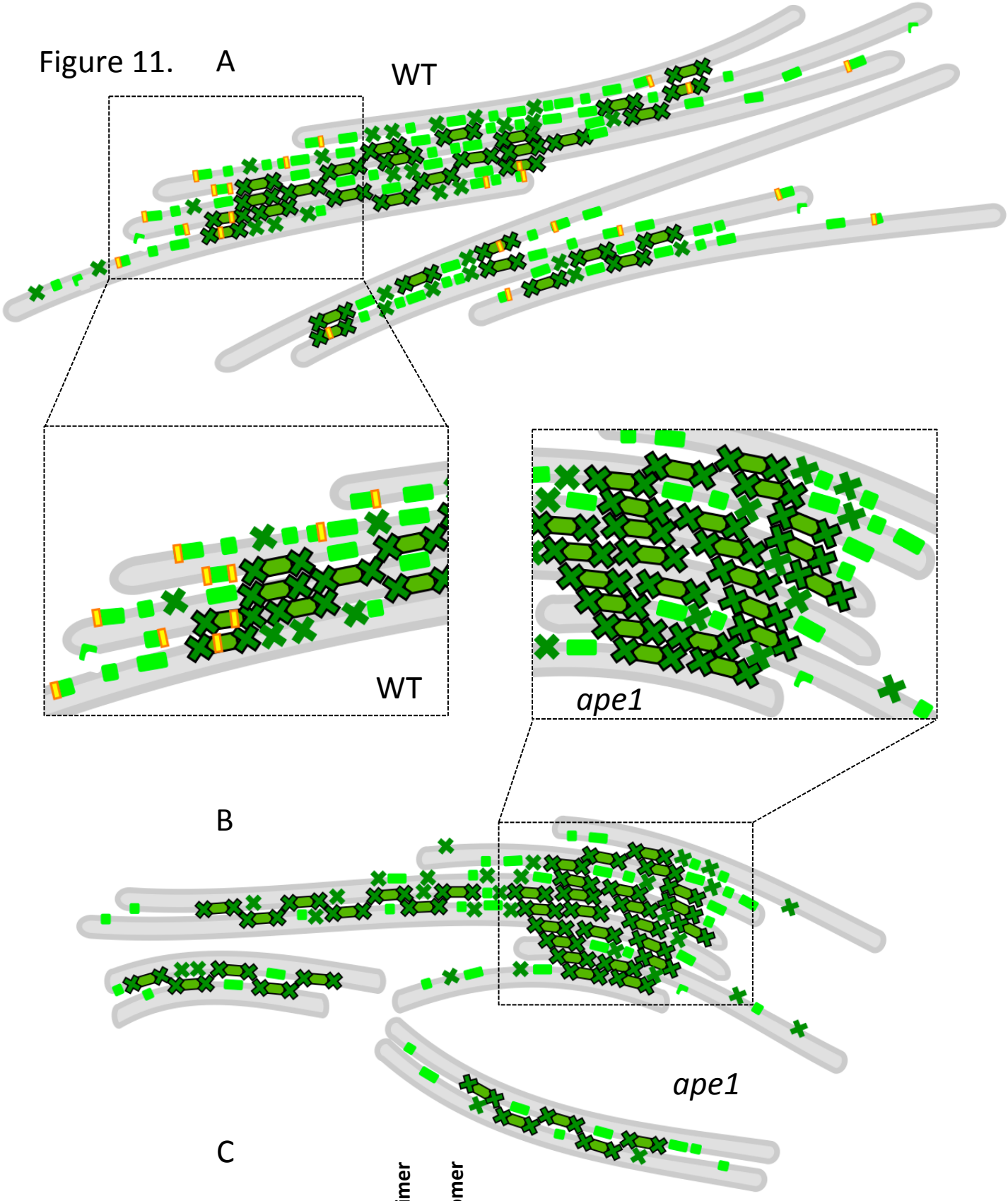

Figure 11. Model: APE1 releases PSII supercomplexes in *Chlamydomonas reinhardtii*. Thylakoid membranes (grey) and lumen (pale grey) harbor PSII of different oligomeric states. (To focus on PSII, other photosynthetic complexes are omitted in this illustration.) **A.** APE1 is bound to PSII core and not LHCII, when in PSII supercomplexes it releases core complexes. PSII complexes are heterogeneous in their oligomeric composition in cells grown phototrophically under ambient CO_2. As a consequence, PSII plasticity influences the stacking of Chlamydomonas thylakoids. **B.** In the absence of APE1, PSII supercomplexes are more stable and interactions between the LHCII influence greater stacking of membranes that lead to a reduction in end-membranes and non-apressed membranes. It also affects the number of PSII cores that are free and not bound to LHCII and the total accumulation of PSII. **C.** An example equation for APE1 function: two PSII complexes plus interaction with APE1 results in PSII core dimer , PSII core monomer with APE1, RC47 + free LHCII

Parsed Citations

Adir, N., Zer, H., Shochat, S., and Ohad, I. (2003). Photoinhibition - a historical perspective. Photosynthesis research 76, 343-370.
Pubmed: Author and Title
Google Scholar: Author Only Title Only Author and Title

Albanese, P., Melero, R., Engel, B.D., Grinzato, A., Berto, P., Manfredi, M., Chiodoni, A., Vargas, J., Sorzano, C.O.S., Marengo, E., et al. (2017). Pea PSII-LHCII supercomplexes form pairs by making connections across the stromal gap. Scientific reports 7, 10067.
Pubmed: Author and Title
Google Scholar: Author Only Title Only Author and Title

Albanese, P., Nield, J., Tabares, J.A., Chiodoni, A., Manfredi, M., Gosetti, F., Marengo, E., Saracco, G., Barber, J., and Pagliano, C. (2016). Isolation of novel PSII-LHCII megacomplexes from pea plants characterized by a combination of proteomics and electron microscopy. Photosynthesis research 130, 19-31.
Pubmed: Author and Title
Google Scholar: Author Only Title Only Author and Title

Anderson, J.M., Chow, W.S., and Goodchild, D.J. (1988). Thylakoid membrane organisation in sun/shade acclimation. . Austr J Plant Physiol 15, 11–26.
Pubmed: Author and Title
Google Scholar: Author Only Title Only Author and Title

Anderson, J.M., Chow, W.S., and Park, Y.I. (1995). The grand design of photosynthesis: Acclimation of the photosynthetic apparatus to environmental cues. Photosynthesis research 46, 129-139.
Pubmed: Author and Title
Google Scholar: Author Only Title Only Author and Title

Aslanidis, C., and de Jong, P.J. (1990). Ligation-independent cloning of PCR products (LIC-PCR). Nucleic acids research 18, 6069-6074.
Pubmed: Author and Title
Google Scholar: Author Only Title Only Author and Title

Baena-Gonzalez, E., and Sheen, J. (2008). Convergent energy and stress signaling. Trends in plant science 13, 474-482.
Pubmed: Author and Title
Google Scholar: Author Only Title Only Author and Title

Bec Kova, M., Yu, J., Krynicka, V., Kozlo, A., Shao, S., Konik, P., Komenda, J., Murray, J.W., and Nixon, P.J. (2017). Structure of Psb29/Thf1 and its association with the FtsH protease complex involved in photosystem II repair in cyanobacteria. Philosophical transactions of the Royal Society of London Series B, Biological sciences 372.
Pubmed: Author and Title
Google Scholar: Author Only Title Only Author and Title

Beck, C., Knoop, H., and Steuer, R. (2018). Modules of co-occurrence in the cyanobacterial pan-genome reveal functional associations between groups of ortholog genes. PLoS genetics 14, e1007239.
Pubmed: Author and Title
Google Scholar: Author Only Title Only Author and Title

Bielczynski, L.W., Schansker, G., and Croce, R. (2016). Effect of Light Acclimation on the Organization of Photosystem II Super- and Sub-Complexes in Arabidopsis thaliana. Frontiers in plant science 7, 105.
Pubmed: Author and Title
Google Scholar: Author Only Title Only Author and Title

Björkman, O., and Ludlow, M.M. (1972). Characterization of the light climate on the floor of a Queensland rainforest. . Carnegie Inst Washington Yearbook 71, 85–94.
Pubmed: Author and Title
Google Scholar: Author Only Title Only Author and Title

Boekema, E.J., van Breemen, J.F., van Roon, H., and Dekker, J.P. (2000). Arrangement of photosystem II supercomplexes in crystalline macrodomains within the thylakoid membrane of green plant chloroplasts. Journal of molecular biology 301, 1123-1133.
Pubmed: Author and Title
Google Scholar: Author Only Title Only Author and Title

Boekema, E.J., van Roon, H., Calkoen, F., Bassi, R., and Dekker, J.P. (1999). Multiple types of association of photosystem II and its light-harvesting antenna in partially solubilized photosystem II membranes. Biochemistry 38, 2233-2239.
Pubmed: Author and Title
Google Scholar: Author Only Title Only Author and Title

Bricker, T.M., and Ghanotakis, D.F. (1996). ntroduction to Oxygen Evolution and the Oxygen-Evolving Complex. In Oxygenic Photosynthesis: The Light Reactions Advances in Photosynthesis and Respiration O. D.R., Y. C.F., and H. I.F., eds. (Dordrecht: Springer).
Pubmed: Author and Title
Google Scholar: Author Only Title Only Author and Title

Caffarri, S., Kouril, R., Kereiche, S., Boekema, E.J., and Croce, R. (2009). Functional architecture of higher plant photosystem II supercomplexes. The EMBO journal 28, 3052-3063.

Pubmed: Author and Title
Google Scholar: Author Only Title Only Author and Title

Caffarri, S., Tibiletti, T., Jennings, R.C., and Santabarbara, S. (2014). A comparison between plant photosystem I and photosystem II architecture and functioning. Current protein & peptide science 15, 296-331.
Pubmed: Author and Title
Google Scholar: Author Only Title Only Author and Title

Chaux, F., Johnson, X., Auroy, P., Beyly-Adriano, A., Te, I., Cuine, S., and Peltier, G. (2017). PGRL1 and LHCSR3 Compensate for Each Other in Controlling Photosynthesis and Avoiding Photosystem I Photoinhibition during High Light Acclimation of Chlamydomonas Cells. Molecular plant 10, 216-218.
Pubmed: Author and Title
Google Scholar: Author Only Title Only Author and Title

Chaux, F., Peltier, G., and Johnson, X. (2015). A security network in PSI photoprotection: regulation of photosynthetic control, NPQ and O2 photoreduction by cyclic electron flow. Frontiers in plant science 6, 875.
Pubmed: Author and Title
Google Scholar: Author Only Title Only Author and Title

Choquet, Y., Wostrikoff, K., Rimbault, B., Zito, F., Girard-Bascou, J., Drapier, D., and Wollman, F.A. (2001). Assembly-controlled regulation of chloroplast gene translation. Biochemical Society transactions 29, 421-426.
Pubmed: Author and Title
Google Scholar: Author Only Title Only Author and Title

Chua, N.H., and Bennoun, P. (1975). Thylakoid membrane polypeptides of Chlamydomonas reinhardtii: wild-type and mutant strains deficient in photosystem II reaction center. Proceedings of the National Academy of Sciences of the United States of America 72, 2175-2179.
Pubmed: Author and Title
Google Scholar: Author Only Title Only Author and Title

Correa-Galvis, V., Poschmann, G., Melzer, M., Stuhler, K., and Jahns, P. (2016a). PsbS interactions involved in the activation of energy dissipation in Arabidopsis. Nature plants 2, 15225.
Pubmed: Author and Title
Google Scholar: Author Only Title Only Author and Title

Correa-Galvis, V., Redekop, P., Guan, K., Griess, A., Truong, T.B., Wakao, S., Niyogi, K.K., and Jahns, P. (2016b). Photosystem II Subunit PsbS Is Involved in the Induction of LHCSR Protein-dependent Energy Dissipation in Chlamydomonas reinhardtii. The Journal of biological chemistry 291, 17478-17487.
Pubmed: Author and Title
Google Scholar: Author Only Title Only Author and Title

Cuni, A., Xiong, L., Sayre, R., Rappaport, F., and Lavergne, J. (2004). Modification of the pheophytin midpoint potential in photosystem II: Modulation of the quantum yield of charge separation and of charge recombination pathways. Physical Chemistry Chemical Physics 6, 4825-4831.
Pubmed: Author and Title
Google Scholar: Author Only Title Only Author and Title

Dang, K.V., Plet, J., Tolleter, D., Jokel, M., Cuine, S., Carrier, P., Auroy, P., Richaud, P., Johnson, X., Alric, J., et al. (2014). Combined increases in mitochondrial cooperation and oxygen photoreduction compensate for deficiency in cyclic electron flow in Chlamydomonas reinhardtii. The Plant cell 26, 3036-3050.
Pubmed: Author and Title
Google Scholar: Author Only Title Only Author and Title

Danielsson, R., Suorsa, M., Paakkarinen, V., Albertsson, P.A., Styring, S., Aro, E.M., and Mamedov, F. (2006). Dimeric and monomeric organization of photosystem II. Distribution of five distinct complexes in the different domains of the thylakoid membrane. The Journal of biological chemistry 281, 14241-14249.
Pubmed: Author and Title
Google Scholar: Author Only Title Only Author and Title

Dent, R.M., Haglund, C.M., Chin, B.L., Kobayashi, M.C., and Niyogi, K.K. (2005). Functional genomics of eukaryotic photosynthesis using insertional mutagenesis of Chlamydomonas reinhardtii. Plant physiology 137, 545-556.
Pubmed: Author and Title
Google Scholar: Author Only Title Only Author and Title

Dinc, E., Ceppi, M.G., Toth, S.Z., Bottka, S., and Schansker, G. (2012). The chl a fluorescence intensity is remarkably insensitive to changes in the chlorophyll content of the leaf as long as the chl a/b ratio remains unaffected. Biochimica et biophysica acta 1817, 770-779.
Pubmed: Author and Title
Google Scholar: Author Only Title Only Author and Title

Drop, B., Webber-Birungi, M., Fusetti, F., Kouril, R., Redding, K.E., Boekema, E.J., and Croce, R. (2011). Photosystem I of Chlamydomonas reinhardtii contains nine light-harvesting complexes (Lhca) located on one side of the core. The Journal of biological chemistry 286, 44878-44887.
Pubmed: Author and Title

Google Scholar: Author Only Title Only Author and Title

Drop, B., Webber-Birungi, M., Yadav, S.K., Filipowicz-Szymanska, A., Fusetti, F., Boekema, E.J., and Croce, R. (2014). Light-harvesting complex II (LHCII) and its supramolecular organization in Chlamydomonas reinhardtii. Biochimica et biophysica acta 1837, 63-72.
Pubmed: Author and Title
Google Scholar: Author Only Title Only Author and Title

Dumas, L., Chazaux, M., Peltier, G., Johnson, X., and Alric, J. (2016). Cytochrome b 6 f function and localization, phosphorylation state of thylakoid membrane proteins and consequences on cyclic electron flow. Photosynthesis research 129, 307-320.
Pubmed: Author and Title
Google Scholar: Author Only Title Only Author and Title

Engel, B.D., Schaffer, M., Kuhn Cuellar, L., Villa, E., Plitzko, J.M., and Baumeister, W. (2015). Native architecture of the Chlamydomonas chloroplast revealed by in situ cryo-electron tomography. eLife 4.
Pubmed: Author and Title
Google Scholar: Author Only Title Only Author and Title

Erickson, E., Wakao, S., and Niyogi, K.K. (2015). Light stress and photoprotection in Chlamydomonas reinhardtii. The Plant journal : for cell and molecular biology 82, 449-465.
Pubmed: Author and Title
Google Scholar: Author Only Title Only Author and Title

Farquhar, G.D., von Caemmerer, S., and Berry, J.A. (1980). A biochemical model of photosynthetic CO2 assimilation in leaves of C 3 species. Planta 149, 78-90.
Pubmed: Author and Title
Google Scholar: Author Only Title Only Author and Title

Fischer, B.B., Dayer, R., Schwarzenbach, Y., Lemaire, S.D., Behra, R., Liedtke, A., and Eggen, R.I. (2009). Function and regulation of the glutathione peroxidase homologous gene GPXH/GPX5 in Chlamydomonas reinhardtii. Plant molecular biology 71, 569-583.
Pubmed: Author and Title
Google Scholar: Author Only Title Only Author and Title

Gonzalez-Ballester, D., de Montaigu, A., Galvan, A., and Fernandez, E. (2005). Restriction enzyme site-directed amplification PCR: a tool to identify regions flanking a marker DNA. Analytical biochemistry 340, 330-335.
Pubmed: Author and Title
Google Scholar: Author Only Title Only Author and Title

Goodenough, U.W., Armstrong, J.J., and Levine, R.P. (1969). Photosynthetic Properties of ac-31, a Mutant Strain of Chlamydomonas reinhardi Devoid of Chloroplast Membrane Stacking. Plant physiology 44, 1001-1012.
Pubmed: Author and Title
Google Scholar: Author Only Title Only Author and Title

Goodenough, U.W., and Levine, R.P. (1969). Chloroplast Ultrastructure in Mutant Strains of Chlamydomonas reinhardi Lacking Components of the Photosynthetic Apparatus. Plant physiology 44, 990-1000.
Pubmed: Author and Title
Google Scholar: Author Only Title Only Author and Title

Goodenough, U.W., and Staehelin, L.A. (1971). Structural differentiation of stacked and unstacked chloroplast membranes. Freeze-etch electron microscopy of wild-type and mutant strains of Chlamydomonas. The Journal of cell biology 48, 594-619.
Pubmed: Author and Title
Google Scholar: Author Only Title Only Author and Title

Guenther, J.E., and Melis, A. (1990). The physiological significance of photosystem II heterogeneity in chloroplasts. Photosynthesis research 23, 105-109.
Pubmed: Author and Title
Google Scholar: Author Only Title Only Author and Title

Harris, E.H. (1989). The Chlamydomonas Sourcebook: A Comprehensive

Guide to Biology and Laboratory Use. (San Diego: Academic Press,).

Heinnickel, M.L., and Grossman, A.R. (2013). The GreenCut: re-evaluation of physiological role of previously studied proteins and potential novel protein functions. Photosynthesis research 116, 427-436.
Pubmed: Author and Title
Google Scholar: Author Only Title Only Author and Title

Herbstová, M., Tietz, S., Kinzel, C., Turkina, M.V., and Kirchhoff, H. (2012). Architectural switch in plant photosynthetic membranes induced by light stress. Proceedings of the National Academy of Sciences 109, 20130-20135.
Pubmed: Author and Title
Google Scholar: Author Only Title Only Author and Title

Huang, W., Chen, Q., Zhu, Y., Hu, F., Zhang, L., Ma, Z., He, Z., and Huang, J. (2013). Arabidopsis thylakoid formation 1 is a critical regulator for dynamics of PSII-LHCII complexes in leaf senescence and excess light. Molecular plant 6, 1673-1691.
Pubmed: Author and Title
Google Scholar: Author Only Title Only Author and Title

Jarvi, S., Suorsa, M., and Aro, E.M. (2015). Photosystem II repair in plant chloroplasts--Regulation, assisting proteins and shared components with photosystem II biogenesis. Biochimica et biophysica acta 1847, 900-909.
Pubmed: Author and Title
Google Scholar: Author Only Title Only Author and Title

Johnson, X., Steinbeck, J., Dent, R.M., Takahashi, H., Richaud, P., Ozawa, S., Houille-Vernes, L., Petroutsos, D., Rappaport, F., Grossman, A.R., et al. (2014). Proton gradient regulation 5-mediated cyclic electron flow under ATP- or redox-limited conditions: a study of DeltaATpase pgr5 and DeltarbcL pgr5 mutants in the green alga Chlamydomonas reinhardtii. Plant physiology 165, 438-452.
Pubmed: Author and Title
Google Scholar: Author Only Title Only Author and Title

Johnson, X., Vandystadt, G., Bujaldon, S., Wollman, F.A., Dubois, R., Roussel, P., Alric, J., and Beal, D. (2009). A new setup for in vivo fluorescence imaging of photosynthetic activity. Photosynthesis research 102, 85-93.
Pubmed: Author and Title
Google Scholar: Author Only Title Only Author and Title

Johnson, X., Wostrikoff, K., Finazzi, G., Kuras, R., Schwarz, C., Bujaldon, S., Nickelsen, J., Stern, D.B., Wollman, F.A., and Vallon, O. (2010). MRL1, a conserved Pentatricopeptide repeat protein, is required for stabilization of rbcL mRNA in Chlamydomonas and Arabidopsis. The Plant cell 22, 234-248.
Pubmed: Author and Title
Google Scholar: Author Only Title Only Author and Title

Kallberg, M., Wang, H., Wang, S., Peng, J., Wang, Z., Lu, H., and Xu, J. (2012). Template-based protein structure modeling using the RaptorX web server. Nature protocols 7, 1511-1522.
Pubmed: Author and Title
Google Scholar: Author Only Title Only Author and Title

Khan, N.Z., Lindquist, E., and Aronsson, H. (2013). New putative chloroplast vesicle transport components and cargo proteins revealed using a bioinformatics approach: an Arabidopsis model. PloS one 8, e59898.
Pubmed: Author and Title
Google Scholar: Author Only Title Only Author and Title

Khatoon, M., Inagawa, K., Pospisil, P., Yamashita, A., Yoshioka, M., Lundin, B., Horie, J., Morita, N., Jajoo, A., Yamamoto, Y., et al. (2009). Quality control of photosystem II: Thylakoid unstacking is necessary to avoid further damage to the D1 protein and to facilitate D1 degradation under light stress in spinach thylakoids. The Journal of biological chemistry 284, 25343-25352.
Pubmed: Author and Title
Google Scholar: Author Only Title Only Author and Title

Kirchhoff, H. (2019). Chloroplast ultrastructure in plants. The New phytologist 223, 565-574.
Pubmed: Author and Title
Google Scholar: Author Only Title Only Author and Title

Komenda, J., and Sobotka, R. (2016). Cyanobacterial high-light-inducible proteins--Protectors of chlorophyll-protein synthesis and assembly. Biochimica et biophysica acta 1857, 288-295.
Pubmed: Author and Title
Google Scholar: Author Only Title Only Author and Title

Koochak, H., Puthiyaveetil, S., Mullendore, D.L., Li, M., and Kirchhoff, H. (2019). The structural and functional domains of plant thylakoid membranes. The Plant journal : for cell and molecular biology 97, 412-429.
Pubmed: Author and Title
Google Scholar: Author Only Title Only Author and Title

Kouril, R., Lukas, N., Semchonok, D.A., Boekema, E.J., and Ilik, P. (2018). Membrane Protein Complexes: Structure and Function. In Subcellular Biochemistry, E.J.B. J. Robin Harris, ed. (Singapore: Springer), p. 459.
Pubmed: Author and Title
Google Scholar: Author Only Title Only Author and Title

Kouril, R., Wientjes, E., Bultema, J.B., Croce, R., and Boekema, E.J. (2013). High-light vs. low-light: effect of light acclimation on photosystem II composition and organization in Arabidopsis thaliana. Biochimica et biophysica acta 1827, 411-419.
Pubmed: Author and Title
Google Scholar: Author Only Title Only Author and Title

Larosa, V., Meneghesso, A., La Rocca, N., Steinbeck, J., Hippler, M., Szabo, I., and Morosinotto, T. (2018). Mitochondria Affect Photosynthetic Electron Transport and Photosensitivity in a Green Alga. Plant physiology 176, 2305-2314.
Pubmed: Author and Title
Google Scholar: Author Only Title Only Author and Title

Li, X., Zhang, R., Patena, W., Gang, S.S., Blum, S.R., Ivanova, N., Yue, R., Robertson, J.M., Lefebvre, P.A., Fitz-Gibbon, S.T., et al. (2016). An Indexed, Mapped Mutant Library Enables Reverse Genetics Studies of Biological Processes in Chlamydomonas reinhardtii. The Plant cell 28, 367-387.
Pubmed: Author and Title
Google Scholar: Author Only Title Only Author and Title

Lu, Y. (2016). Identification and Roles of Photosystem II Assembly, Stability, and Repair Factors in Arabidopsis. Frontiers in plant

science 7, 168.
Pubmed: Author and Title
Google Scholar: Author Only Title Only Author and Title

Majeran, W., Zybailov, B., Ytterberg, A.J., Dunsmore, J., Sun, Q., and van Wijk, K.J. (2008). Consequences of C4 differentiation for chloroplast membrane proteomes in maize mesophyll and bundle sheath cells. Molecular & cellular proteomics : MCP 7, 1609-1638.
Pubmed: Author and Title
Google Scholar: Author Only Title Only Author and Title

Melis, A. (1991). Dynamics of photosynthetic membrane composition and function. Biochimica et biophysica acta 1058, 87–106.
Pubmed: Author and Title
Google Scholar: Author Only Title Only Author and Title

Melis, A. (1996). Excitation energy transfer: functional and dynamic

aspects of Lhc (cab) proteins. In Oxygenic Photosynthesis: The Light Reactions

Volume 4 of Advances in Photosynthesis and Respiration, D.R. Ort, and C.F. Yocum, eds. (Dordrecht, The Netherlands: Kluwer Academic Publishers), pp. 523–538.
Pubmed: Author and Title
Google Scholar: Author Only Title Only Author and Title

Melis, A., and Homann, P.H. (1976). Heterogeneity of the Photochemical centres in system II of Chloroplasts Photochemistry and Photobiology 23, 343-350.
Pubmed: Author and Title
Google Scholar: Author Only Title Only Author and Title

Merchant, S.S., Prochnik, S.E., Vallon, O., Harris, E.H., Karpowicz, S.J., Witman, G.B., Terry, A., Salamov, A., Fritz-Laylin, L.K., Marechal-Drouard, L., et al. (2007). The Chlamydomonas genome reveals the evolution of key animal and plant functions. Science 318, 245-250.
Pubmed: Author and Title
Google Scholar: Author Only Title Only Author and Title

Michaeli, S., Honig, A., Levanony, H., Peled-Zehavi, H., and Galili, G. (2014). Arabidopsis ATG8-INTERACTING PROTEIN1 is involved in autophagy-dependent vesicular trafficking of plastid proteins to the vacuole. The Plant cell 26, 4084-4101.
Pubmed: Author and Title
Google Scholar: Author Only Title Only Author and Title

Mulkidjanian, A.Y., Koonin, E.V., Makarova, K.S., Mekhedov, S.L., Sorokin, A., Wolf, Y.I., Dufresne, A., Partensky, F., Burd, H., Kaznadzey, D., et al. (2006). The cyanobacterial genome core and the origin of photosynthesis. Proceedings of the National Academy of Sciences of the United States of America 103, 13126-13131.
Pubmed: Author and Title
Google Scholar: Author Only Title Only Author and Title

Munekage, Y.N., Genty, B., and Peltier, G. (2008). Effect of PGR5 impairment on photosynthesis and growth in Arabidopsis thaliana. Plant & cell physiology 49, 1688-1698.
Pubmed: Author and Title
Google Scholar: Author Only Title Only Author and Title

Muranaka, L.S., Rutgers, M., Bujaldon, S., Heublein, A., Geimer, S., Wollman, F.A., and Schroda, M. (2016). TEF30 Interacts with Photosystem II Monomers and Is Involved in the Repair of Photodamaged Photosystem II in Chlamydomonas reinhardtii. Plant physiology 170, 821-840.
Pubmed: Author and Title
Google Scholar: Author Only Title Only Author and Title

Myouga, F., Takahashi, K., Tanaka, R., Nagata, N., Kiss, A.Z., Funk, C., Nomura, Y., Nakagami, H., Jansson, S., and Shinozaki, K. (2018). Stable Accumulation of Photosystem II Requires ONE-HELIX PROTEIN1 (OHP1) of the Light Harvesting-Like Family. Plant physiology 176, 2277-2291.
Pubmed: Author and Title
Google Scholar: Author Only Title Only Author and Title

Nawrocki, W.J., Liu, X., and Croce, R. (2020). Chlamydomonas reinhardtii Exhibits De Facto Constitutive NPQ Capacity in Physiologically Relevant Conditions. Plant physiology 182, 472-479.
Pubmed: Author and Title
Google Scholar: Author Only Title Only Author and Title

Pagliano, C., Barera, S., Chimirri, F., Saracco, G., and Barber, J. (2012). Comparison of the alpha and beta isomeric forms of the detergent n-dodecyl-D-maltoside for solubilizing photosynthetic complexes from pea thylakoid membranes. Biochimica et biophysica acta 1817, 1506-1515.
Pubmed: Author and Title
Google Scholar: Author Only Title Only Author and Title

Plochinger, M., Schwenkert, S., von Sydow, L., Schroder, W.P., and Meurer, J. (2016). Functional Update of the Auxiliary Proteins PsbW, PsbY, HCF136, PsbN, TerC and ALB3 in Maintenance and Assembly of PSII. Frontiers in plant science 7, 423.
Pubmed: Author and Title
Google Scholar: Author Only Title Only Author and Title

Polukhina, I., Fristedt, R., Dinc, E., Cardol, P., and Croce, R. (2016). Carbon Supply and Photoacclimation Cross Talk in the Green Alga Chlamydomonas reinhardtii. Plant physiology 172, 1494-1505.
Pubmed: Author and Title
Google Scholar: Author Only Title Only Author and Title

Pribil, M., Labs, M., and Leister, D. (2014). Structure and dynamics of thylakoids in land plants. J Exp Bot 65, 1955-1972.
Pubmed: Author and Title
Google Scholar: Author Only Title Only Author and Title

Pribil, M., Sandoval-Ibanez, O., Xu, W., Sharma, A., Labs, M., Liu, Q., Galgenmuller, C., Schneider, T., Wessels, M., Matsubara, S., et al. (2018). Fine-Tuning of Photosynthesis Requires CURVATURE THYLAKOID1-Mediated Thylakoid Plasticity. Plant physiology 176, 2351-2364.
Pubmed: Author and Title
Google Scholar: Author Only Title Only Author and Title

Rexroth, S., Meyer zu Tittingdorf, J.M., Krause, F., Dencher, N.A., and Seelert, H. (2003). Thylakoid membrane at altered metabolic state: challenging the forgotten realms of the proteome. Electrophoresis 24, 2814-2823.
Pubmed: Author and Title
Google Scholar: Author Only Title Only Author and Title

Rexroth, S., Mullineaux, C.W., Ellinger, D., Sendtko, E., Rogner, M., and Koenig, F. (2011). The plasma membrane of the cyanobacterium Gloeobacter violaceus contains segregated bioenergetic domains. The Plant cell 23, 2379-2390.
Pubmed: Author and Title
Google Scholar: Author Only Title Only Author and Title

Roach, T., Baur, T., Stoggl, W., and Krieger-Liszkay, A. (2017). Chlamydomonas reinhardtii responding to high light: a role for 2-propenal (acrolein). Physiologia plantarum 161, 75-87.
Pubmed: Author and Title
Google Scholar: Author Only Title Only Author and Title

Rochaix, J.D. (2014). Regulation and dynamics of the light-harvesting system. Annual review of plant biology 65, 287-309.
Pubmed: Author and Title
Google Scholar: Author Only Title Only Author and Title

Rozak, P.R., Seiser, R.M., Wacholtz, W.F., and Wise, R.R. (2002). Rapid, reversible alterations in spinach thylakoid appression upon changes in light intensity. Plant, Cell and Environment 25, 421-429.
Pubmed: Author and Title
Google Scholar: Author Only Title Only Author and Title

Schroda, M., Beck, C.F., and Vallon, O. (2002). Sequence elements within an HSP70 promoter counteract transcriptional transgene silencing in Chlamydomonas. The Plant journal : for cell and molecular biology 31, 445-455.
Pubmed: Author and Title
Google Scholar: Author Only Title Only Author and Title

Schwarz, E.M., Tietz, S., and Froehlich, J.E. (2018). Photosystem I-LHCII megacomplexes respond to high light and aging in plants. Photosynthesis research 136, 107-124.
Pubmed: Author and Title
Google Scholar: Author Only Title Only Author and Title

Semchonok, D.A., Sathish Yadav, K.N., Xu, P., Drop, B., Croce, R., and Boekema, E.J. (2017). Interaction between the photoprotective protein LHCSR3 and C2S2 Photosystem II supercomplex in Chlamydomonas reinhardtii. Biochimica et biophysica acta Bioenergetics 1858, 379-385.
Pubmed: Author and Title
Google Scholar: Author Only Title Only Author and Title

Shen, L., Huang, Z., Chang, S., Wang, W., Wang, J., Kuang, T., Han, G., Shen, J.R., and Zhang, X. (2019). Structure of a C2S2M2N2-type PSII-LHCII supercomplex from the green alga Chlamydomonas reinhardtii. Proceedings of the National Academy of Sciences of the United States of America 116, 21246-21255.
Pubmed: Author and Title
Google Scholar: Author Only Title Only Author and Title

Shi, L.X., Hall, M., Funk, C., and Schroder, W.P. (2012). Photosystem II, a growing complex: updates on newly discovered components and low molecular mass proteins. Biochimica et biophysica acta 1817, 13-25.
Pubmed: Author and Title
Google Scholar: Author Only Title Only Author and Title

Sizova, I., Fuhrmann, M., and Hegemann, P. (2001). A Streptomyces rimosus aphVIII gene coding for a new type phosphotransferase provides stable antibiotic resistance to Chlamydomonas reinhardtii. Gene 277, 221-229.
Pubmed: Author and Title
Google Scholar: Author Only Title Only Author and Title

Stark, H. (2010). GraFix: stabilization of fragile macromolecular complexes for single particle cryo-EM. Methods in enzymology 481, 109-126.
Pubmed: Author and Title

Google Scholar: Author Only Title Only Author and Title

Su, X., Ma, J., Wei, X., Cao, P., Zhu, D., Chang, W., Liu, Z., Zhang, X., and Li, M. (2017). Structure and assembly mechanism of plant C2S2M2-type PSII-LHCII supercomplex. Science 357, 815-820.
Pubmed: Author and Title
Google Scholar: Author Only Title Only Author and Title

Suorsa, M., Rantala, M., Mamedov, F., Lespinasse, M., Trotta, A., Grieco, M., Vuorio, E., Tikkanen, M., Jarvi, S., and Aro, E.M. (2015). Light acclimation involves dynamic re-organization of the pigment-protein megacomplexes in non-appressed thylakoid domains. The Plant journal : for cell and molecular biology 84, 360-373.
Pubmed: Author and Title
Google Scholar: Author Only Title Only Author and Title

Terashima, M., Specht, M., and Hippler, M. (2011). The chloroplast proteome: a survey from the Chlamydomonas reinhardtii perspective with a focus on distinctive features. Current genetics 57, 151-168.
Pubmed: Author and Title
Google Scholar: Author Only Title Only Author and Title

Theis, J., and Schroda, M. (2016). Revisiting the photosystem II repair cycle. Plant Signaling & Behavior 11, e1218587.
Pubmed: Author and Title
Google Scholar: Author Only Title Only Author and Title

Thornton, L.E., Ohkawa, H., Roose, J.L., Kashino, Y., Keren, N., and Pakrasi, H.B. (2004). Homologs of plant PsbP and PsbQ proteins are necessary for regulation of photosystem ii activity in the cyanobacterium Synechocystis 6803. The Plant cell 16, 2164-2175.
Pubmed: Author and Title
Google Scholar: Author Only Title Only Author and Title

Tibiletti, T., Auroy, P., Peltier, G., and Caffarri, S. (2016). Chlamydomonas reinhardtii PsbS Protein Is Functional and Accumulates Rapidly and Transiently under High Light. Plant physiology 171, 2717-2730.
Pubmed: Author and Title
Google Scholar: Author Only Title Only Author and Title

Tomizioli, M., Lazar, C., Brugiere, S., Burger, T., Salvi, D., Gatto, L., Moyet, L., Breckels, L.M., Hesse, A.M., Lilley, K.S., et al. (2014). Deciphering thylakoid sub-compartments using a mass spectrometry-based approach. Molecular & cellular proteomics : MCP 13, 2147-2167.
Pubmed: Author and Title
Google Scholar: Author Only Title Only Author and Title

Torabi, S., Umate, P., Manavski, N., Plochinger, M., Kleinknecht, L., Bogireddi, H., Herrmann, R.G., Wanner, G., Schroder, W.P., and Meurer, J. (2014). PsbN is required for assembly of the photosystem II reaction center in Nicotiana tabacum. The Plant cell 26, 1183-1199.
Pubmed: Author and Title
Google Scholar: Author Only Title Only Author and Title

Tyystjarvi, E., and Aro, E.M. (1996). The rate constant of photoinhibition, measured in lincomycin-treated leaves, is directly proportional to light intensity. Proceedings of the National Academy of Sciences of the United States of America 93, 2213-2218.
Pubmed: Author and Title
Google Scholar: Author Only Title Only Author and Title

Umena, Y., Kawakami, K., Shen, J.R., and Kamiya, N. (2011). Crystal structure of oxygen-evolving photosystem II at a resolution of 1.9 A. Nature 473, 55-60.
Pubmed: Author and Title
Google Scholar: Author Only Title Only Author and Title

Walters, R.G. (2005). Towards an understanding of photosynthetic acclimation. J Exp Bot 56, 435-447.
Pubmed: Author and Title
Google Scholar: Author Only Title Only Author and Title

Walters, R.G., Shephard, F., Rogers, J.J., Rolfe, S.A., and Horton, P. (2003). Identification of mutants of Arabidopsis defective in acclimation of photosynthesis to the light environment. Plant physiology 131, 472-481.
Pubmed: Author and Title
Google Scholar: Author Only Title Only Author and Title

Wang, L., Yamano, T., Takane, S., Niikawa, Y., Toyokawa, C., Ozawa, S.I., Tokutsu, R., Takahashi, Y., Minagawa, J., Kanesaki, Y., et al. (2016). Chloroplast-mediated regulation of CO2-concentrating mechanism by Ca2+-binding protein CAS in the green alga Chlamydomonas reinhardtii. Proceedings of the National Academy of Sciences of the United States of America 113, 12586-12591.
Pubmed: Author and Title
Google Scholar: Author Only Title Only Author and Title

Wei, X., Su, X., Cao, P., Liu, X., Chang, W., Li, M., Zhang, X., and Liu, Z. (2016). Structure of spinach photosystem II-LHCII supercomplex at 3.2 A resolution. Nature 534, 69-74.
Pubmed: Author and Title
Google Scholar: Author Only Title Only Author and Title

Yang, D.H., Webster, J., Adam, Z., Lindahl, M., and Andersson, B. (1998). Induction of acclimative proteolysis of the light-harvesting

chlorophyll a/b protein of photosystem II in response to elevated light intensities. Plant physiology 118, 827-834.
Pubmed: Author and Title
Google Scholar: Author Only Title Only Author and Title

Zehr, J.P., Bench, S.R., Carter, B.J., Hewson, I., Niazi, F., Shi, T., Tripp, H.J., and Affourtit, J.P. (2008). Globally distributed uncultivated oceanic N2-fixing cyanobacteria lack oxygenic photosystem II. Science 322, 1110-1112.
Pubmed: Author and Title
Google Scholar: Author Only Title Only Author and Title

Zhang, R., Patena, W., Armbruster, U., Gang, S.S., Blum, S.R., and Jonikas, M.C. (2014). High-Throughput Genotyping of Green Algal Mutants Reveals Random Distribution of Mutagenic Insertion Sites and Endonucleolytic Cleavage of Transforming DNA. The Plant cell 26, 1398-1409.
Pubmed: Author and Title
Google Scholar: Author Only Title Only Author and Title